UNIVERSIDADE D
COIMBRA

Guilherme da Costa Gomes Rodrigues Catela

INFLUENCE OF ARTIFICIAL SALIVA ON THE MECHANICAL PROPERTIES OF SANDWICH STRUCTURES PROCESSED THROUGH ADDITIVE MANUFACTURING

Dissertation under the Integrated Master Degree in Mechanical Engineering, field of speciality in Manufacturing and Project, supervised by Professor Ana Paula da Fonseca Piedade and presented to the Department of Mechanical Engineering from the Faculty of Science and Technology of the University of Coimbra

February of 2021

1 2 9 0

FACULDADE DE CIÊNCIAS E TECNOLOGIA
UNIVERSIDADE D COIMBRA

Influence of Artificial Saliva on the Mechanical Properties of Sandwich Structures processed through Additive Manufacturing

Submitted in Partial Fulfilment of the Requirements for the master degree in Mechanical Engineering in the speciality of Production and Project.

Influência da Saliva Artificial nas Propriedades Mecânicas de Estruturas *Sandwich* processadas por Fabrico Aditivo

Author

Guilherme da Costa Gomes Rodrigues Catela

Advisor

Professora Doutora Ana Paula da Fonseca Piedade

Jury

President	**Doutora Ana Catarina da Silva Pinho** **Researcher in University of Coimbra**
Vowel	**Professor Doutor Fernando Jorge Ventura Antunes** **Auxiliary Professor in University of Coimbra**
Advisor	**Professora Doutora Ana Paula da Fonseca Piedade** **Auxiliary Professor in University of Coimbra**

Coimbra, February of 2021

"*Do not think that what is hard for you to master is humanly impossible; and if it is humanly possible, consider it to be within your reach."*

Marcus Aurelius

ACKNOWLEDGEMENTS

Firstly, I would like to thank my advisor, Professora Doutora Ana Paula da Fonseca Piedade, for all the patience and support she had with me during this work.

To Doutora Ana Catarina Pinho for her friendliness, teachings, support, and disposal needed to conclude this work.

To everyone else in the work group that helped me achieve my goal,

To my colleagues, who I always strived to catch up after falling behind too many times. My motivation was always to reach the same heights you have reached.

To my friends, who were always supportive of my decisions, and ensured I was diligent about my work, staying focused, but enjoying the spare time as well.

To my family, for the continued support along this moment of my life.

To Sara, whose support was critical to the conclusion of this work. I thank you for the patience and love you have shown me all these years. I thank you as well for being a role-model of mine when it comes to discipline and diligence.

Abstract

With the advances in technology, Additive Manufacturing (AM) processes have been gaining an increased importance in the world of industry when compared to other manufacturing processes. This is due to the fact that AM is able to produce parts and components with complex geometries unachievable by other technologies, while generating little or no waste during and after production. When compared to other manufacturing processes, AM uses less raw material, which lowers the production costs. The high importance of these factors overcome the drawbacks that are sometimes associated with the quality of the surface finish and geometry tolerance of printed parts. Nowadays, AM processes have the opportunity to have an impact in the manufacturing world, being a core element of the Industry 4.0.

From every available process used in Additive Manufacturing, Fused Deposition Modelling (FDM), commonly known as 3D Printing, is the one which requires the less amount of equipment, and is one of the easiest, if not the easiest to use of all processes, and the equipment needed to produce parts, components or devices through this process are easily available.

The main topic of this dissertation is the use of this technology with the aim of producing mouthguards for athletes. The current processes to create mouthguards do not produce devices with the adequate design and customized production has a high cost. The materials used have some hindrances associated with them, and the technologies used in the processing produce a high amount of waste. Through FDM processing, it is possible to obtain completely customized mouthguards with minimal waste. There is also the focus on the comprehension of which material and material combination will suit better this application, in order to have a reliable substitute for the current material employed in the production of mouthguards, which is EVA – copolymer of ethylene-vinyl acetate.

The used materials were the copolymer Acrylonitrile-Butadiene-Styrene (ABS), High Impact Polystyrene (HIPS), Poly(methyl methacrylate) (PMMA) and Thermoplastic Polyurethane (TPU). The influence of the use on the mechanical properties was also evaluated through an aging process with an artificial saliva solution. For both mono and

sandwich multi-material combinations, before and after the saliva influence, the mechanical properties were evaluated through Transverse Impact Testing and Flexural Testing (Three-Point Bending – 3PB). The tested specimens were printed according to the standards ASTM D790 and Charpy ISO179.

Keywords Additive Manufacturing, 3D Printing, Mouthguard, Multi-material Printing, Sandwich Structures

Resumo

Com o desenvolvimento tecnológico, os processos de Fabrico Aditivo têm alcançado uma importância acrescida no mundo da indústria quando comparados com outros processos de fabrico. Tal é devido ao facto de para além de serem capazes de produzir estruturas tridimensionais complexas, que não são obtidas por nenhuma outra tecnologia, também o processo produz uma quantidade mínima, ou mesmo nula, de desperdício. A quantidade de matéria-prima que é utilizada é menor quando comparada com outros processos, o que leva à produção de partes, componentes e dispositivos mais económicos. Estes fatores têm uma elevada importância, de tal forma que se sobrepõem a algumas desvantagens associadas, em alguns casos, como à qualidade do acabamento superficial e à tolerância geométrica. Atualmente, os processos de Fabrico Aditivo têm a oportunidade de criar impacto no mundo da produção, sendo um elemento fulcral da Indústria 4.0

De todas as tecnologias associada ao fabrico aditivo, a Modelagem por Deposição Fundida (*Fused Deposition Modeling* – FDM), comummente designada por Impressão 3D, é a mais fácil de utilizar, e que requere equipamentos mais acessíveis e de fácil aquisição.

Esta dissertação centra-se na utilização desta tecnologia na produção de protetores bocais para atletas. O processo atual de produção destes dispositivos não utiliza um *design* adequado, e a produção personalizada envolve um elevado custo. Através do fabrico por FDM, é possível produzir protetores bocais completamente personalizados, por um custo muito menor e com um mínimo de desperdício. Um dos outros objetivos é a utilização de mono ou multi-materiais poliméricos que possam ser substitutos adequados ao material que atualmente é utilizado na produção de protetores bocais, EVA – copolímero de Acetato- de Vinilo de Etileno.

Os materiais que foram objeto de estudo desta dissertação foram o copolímero Acrilonitrilo Butadieno Estireno (ABS), Poliestireno de Elevado Impacto (HIPS), Poli(metil metacrilato) (PMMA) e a Poliuretana Termoplástica (TPU). A variação das propriedades mecânicas com a utilização dos dispositivos foi avaliada através do envelhecimento com uma solução de saliva artificial. As propriedades mecânicas foram avaliadas através de testes de Impacto Transversal e testes de Flexão em Três Pontos (Three Point Bending - 3PB) em

provetes impressos em mono e em multi-material (estruturas sandwich), antes e após o processo de envelhecimento em saliva artificial. Os provetes testados foram impressos segundo as normas ASTM D790 e Charpy ISO179.

Palavras-chave: Fabrico Aditivo, Impressão 3D, Protetores Bucais, Impressão Multi-material, Estruturas Sandwich

Contents

LIST OF FIGURES

LIST OF TABLES

LIST OF SYMBOLS AND ACRONYMS/ ABBREVIATIONS

List of Symbols

b – Width of the specimen

E – Elastic Modulus

h – Thickness/depth of the specimen

I – Momentum of Inertia

L – Span between supports

P – Applied load

T_g – Glass transition temperature

σ – Bending stress

σ_{MAX} – Maximum bending stress

ε – Strain

Acronyms/Abbreviations

3D – Three-Dimensional

3DP – Three-Dimensional Printing

3PB – Three-point Bending

ABS – Acrylonitrile Butadiene Styrene

ADA – American Dental Association

AM – Additive Manufacturing

ASTM – American Society for Testing and Materials

CAD – Computer Aided Design

DED – Direct Energy Deposition

DEM – Departamento de Engenharia Mecânica

DSC – Differential Scanning Calorimetry

EVA – Copolymer of Ethylene-vinyl Acetate

FCTUC – Faculdade de Ciências e Tecnologia da Universidade de Coimbra

FDM – Fused Deposition Modelling

FTIR – Fourier Transform Infrared Spectroscopy

HEX – Hexagonal

HIPS – High Impact Polystyrene

ISO – International Organization for Standardization

LIN – Linear

LOM – Laminated Object Manufacturing

PB – Polybutadiene

PLA – Poly(lactic acid)

PMMA – Poly(methyl methacrylate)

PVA – Poly(vinyl alcohol)

SLA – Stereolithography

SLM – Selective Laser Melting

SLS – Selective Laser Sintering

SM – Subtractive Manufacturing

TGA – Thermogravimetric Analysis

TPU – Thermoplastic Polyurethane

INTRODUCTION

Additive Manufacturing (AM) is an increasingly present reality in the industry due to technological advances. The stage where these processing methods were applied to produce prototypes has rapidly evolved to one where functional components and parts are processed, with applications in many fields. Moreover, there is an increase in the opportunities for the development of products, which can present advantages due to being processed through AM. One example of these fields is health.

Mouthguards are devices used by athletes to absorb and dissipate energy from impacts the athlete is subject to during the physical activity. They can minimize or prevent injuries to the teeth and surrounding areas of the mouth and jaw.

Previous works have shown that, in a first approach, there is still room to improve and optimize mouthguard production. They must have enough thickness to protect from the impacts previously stated, without compromising the comfort for the wearer. Studies suggest that most athletes prefer not to use conventional mouthguards due to comfort issues.

Usually, mouthguards are produced with a single polymer, EVA - Copolymer of Ethylene-vinyl Acetate, and processed using conventional techniques, which generates waste, and it becomes expensive if customized. EVA has other limitations, such as a low rigidity, which may lead to a worse distribution of the stress from impact, and it absorbs liquids from the mouth, which may impact the geometry of the mouthguard and compromising the retention of it. These allow testing if Fused Deposition Modelling (FDM) is useful in this case. Through FDM, it is possible to produce customized mouthguards efficiently, with no generation of waste and a reduced cost.

It was shown that replacing EVA with a single polymer is not an adequate solution, which is why this work approaches the perspective of using polymeric multi-materials to achieve the exposed needs.

This dissertation is composed of three chapters. The first chapter presents the state of the art and a brief review of the most common AM techniques, focusing on FDM processing and the materials used for said techniques. The second chapter describes the materials used and the experimental methodologies, from printing to testing. The third

chapter presents the results and the discussion regarding these. Conclusions and future perspectives are also presented and all used references.

1. LITERATURE REVIEW

Over the last 50 years, a fast and continuous progress in the manufacturing industry was achieved due to all advances in manufacturing processes [1]. These manufacturing processes can be divided into two major groups: subtractive manufacturing (SM) and additive manufacturing (AM). The first one creates a 3D solid by removing the excess of bulk material through machine cutting. In the other hand, AM is a term that define all the manufacturing methods in which material is added successively, by layers, to create three-dimensional parts[2]–[5]. The production of complex geometries is achievable; however, it has some drawbacks associated to the quality of surface finish and geometry tolerance [6]. AM also stands out when compared to other modern techniques of manufacturing because of its wide range of materials that can be used such as plastics, ceramics, metal alloys and bio-materials [7]. During the model fabrication for any AM techniques, the waste material was found to be minimal compared with SM. Due to the society's environmental concerns, AM techniques turned into a very attractive manufacturing method. Furthermore, more economical models can be fabricated since the amount of raw material is lower than SM [8]. Nowadays, AM has the opportunity to have an impact on the manufacturing world, being a core element of the Industry 4.0 [9].

1.1. Additive Manufacturing

Additive manufacturing (AM), also known as 3D printing, is defined as a process of adding materials to fabricate objects from Computer Aided Design (CAD) models in successive layers. Over the span of more than 20 years, several new AM techniques have been developed and optimized with applications in aerospace, automotive, biomedical, digital art and architectural design [10]. Additive Manufacturing involves various techniques, materials and equipment [11]. In addition, AM of powders by Selective Laser Sintering (SLS), Selective Laser Melting (SLM) or liquid binding in three-dimensional printing, as well as inkjet printing, contour crafting, Stereolithography (SLA) , Direct Energy Deposition (DED) and Laminated Object Manufacturing (LOM) are one of the major

methods of additive manufacturing [12]. However, the most common technique of additive manufacturing is Fused Deposition Modelling (FDM) which uses thermoplastics or polymer-based composites as filament material [13]. These methods are explained in the following subsections as well as their applications and suitable materials for each method, their benefits, and drawbacks.

1.1.1. Powder Bed Fusion (SLS and SLM)

In Powder Bed Fusion processes, thin layers of very fine powders are spread and closely packed on a platform. Through a laser beam or a binder, those powders (in each layers) are fused together [12]. For the following layers, the powders are spread on top of previous layers and fused together, until the final 3D part is printed. Then, the excess of powder is removed by vacuum. Moreover, further processing and detailing such as coating, sintering or infiltration could be employed. The density of the printed part is determined by powder size distribution and packing, being the most crucial factors to the efficacy of this method [14]. The laser can be applied for powders with a low melting/sintering temperature, whereas a liquid binder should then be used. Both Selective Laser Sintering (SLS) and Selective Laser Melting (SLM) operate on the same principle [15]. SLS can be used for a range of polymers, metals and alloy powders. However, SLM can only be applied for certain metals, for example, steel and aluminium. In SLS, the laser scanning does not entirely melt the powders. Furthermore, the high local temperature on the surface of the grains leads the fusion of the powders at the molecular level. However, in SLM, the powders are fully melted and fused together after laser scanning, resulting in in superior mechanical properties [16].

1.1.2. Inkjet Printing

This method is one of the main AM techniques of ceramics. Complex and advanced ceramic structures for applications such as scaffolds for tissue engineering can be printed with this technique. Via the injection nozzle, a stable ceramic suspension is pumped and deposited in the form of droplets onto the substrate [17]. A continuous patter is formed by the droplets. It solidifies to enough strength to hold successive layers of printed materials. Inkjet printing method is efficient and fast, which allows the design of complex structures.

1.1.3. Stereolithography (SLA)

Developed in 1986, SLA was the first methods of additive manufacturing [18]. To initiate a chain reaction on a layer of resin or monomer solution, this technique uses UV light (or electron beam). After activation (radicalisation), the UV-active monomers (mainly acrylic or epoxy-based) instantly convert to polymer chains. After polymerization, a pattern inside the resin layer is solidified in order to hold the subsequent layers. After the conclusion of printing, the unreacted resin is removed. In order to achieve the desired mechanical performance, post-process treatment such as heating, or photo-curing is often used for printed parts. Ceramic-polymer composites [19] or polymer-derived ceramifiable monomers (e.g. silicon oxycarbide [20]) can be printed by using a dispersion of ceramic particles in monomers. High-quality parts at a fine resolution (10 μm) can be printed using this technique [21]. However, it is a slow and expensive process. Furthermore, the range of printing materials is very limited. Additionally, the kinetics of the reaction and. the curing process are complex. Regarding the control of the thickness of each layer, the main factors are the energy of the light source and exposure [18]. The additive manufacturing of complex nanocomposites can be successfully done by this technique [22].

1.1.4. Laminated Object Manufacturing (LOM)

Laminated Object Manufacturing (LOM), one of the first commercially available AM techniques, is based on layer-by-layer cutting and lamination of sheets or rolls of materials. Using a mechanical cutter or laser, successive layers are cut with precision and then bonded together (form-then-bond) or vice versa (bond- then-form). The form-then-bond method is used particularly for thermal bonding ceramics and metallic materials. By removing excess materials before bonding, this method facilitates the construction of internal features [23], [24]. After cutting, the excess materials are left for printing support and, when the process is completed, they can be removed and recycled [25]. Polymer composites, ceramics, paper and metal-filled tapes can be used in LOM. Depending on the type of materials and desired properties, post-processing (such as high-temperature treatment) can be recommended. Several industries such as paper manufacturing, foundry industries, electronics and smart structures use LOM. This additive manufacturing technique can result in a reduction of tooling cost and manufacturing time and is considered one of the best AM techniques for

larger structures. Despite these benefits, LOM models present inferior surface quality when not post-processed. Furthermore, when compared to powder-bed methods, LOM has lower dimensional accuracy and the elimination of the excess parts of laminates after formation of the object is time-consuming. The presented technique is not recommended for complex shapes [10], [12].

1.1.5. Fused Deposition Modelling (FDM)

Fused Deposition Modelling (FDM), commonly called 3D printing, is a method in which a continuous filament of a thermoplastic polymer is used to 3D print layers of materials. A digital model must be created through a CAD software to print parts and components via FDM. This software allows for the creation of models with the desired geometry [10]. In the FDM process, the material, in the form of a filament, is heated at the nozzle to reach the desired viscosity. Then, it is extruded on the platform or on the previously printed layers. This deposition of the heated viscous material completes as many cycles as needed to create the intended part or component. It is possible to print parts and components from thermoplastic filaments through this method [26]. It is important to notice that the thermoplasticity of the polymer filament is an essential property for FDM. This property allows the filaments to fuse together during printing and subsequently to solidify after printing, at room temperature. The main processing parameters that affect the mechanical properties of printed parts are the layer thickness, width and orientation of filaments and air gap (in the same layer or between layers) [13]. The leading cause of mechanical weakness was found to be the inter-layer distortion [27]. FDM benefits of being a low-cost, high speed and relatively simple process. However, FDM has some drawbacks such as weak mechanical properties, layer-by-layer appearance and sometimes poor surface quality [28]. In addition, for this technique there are a limited number of thermoplastic materials [13]. The enhancement of the mechanical properties of 3D printed parts was achieved by the development of fibre-reinforced composites using FDM [29]. However and regarding this last topic, fibre orientation, bonding between the fibre and matrix and void formation are the main challenges that arise in 3D printed composite parts [21], [29]. This method has the advantage of having the capacity of printing parts in multi-materials [16]. With this, it is possible to print parts with complex geometries, where a soluble material like poly(vinyl

alcohol) (PVA), with lower mechanical properties is used as a support for said parts. After the part has been created, the support material can be easily removed [31], [32].

Figure 1.1 shows an illustration of the FDM process.

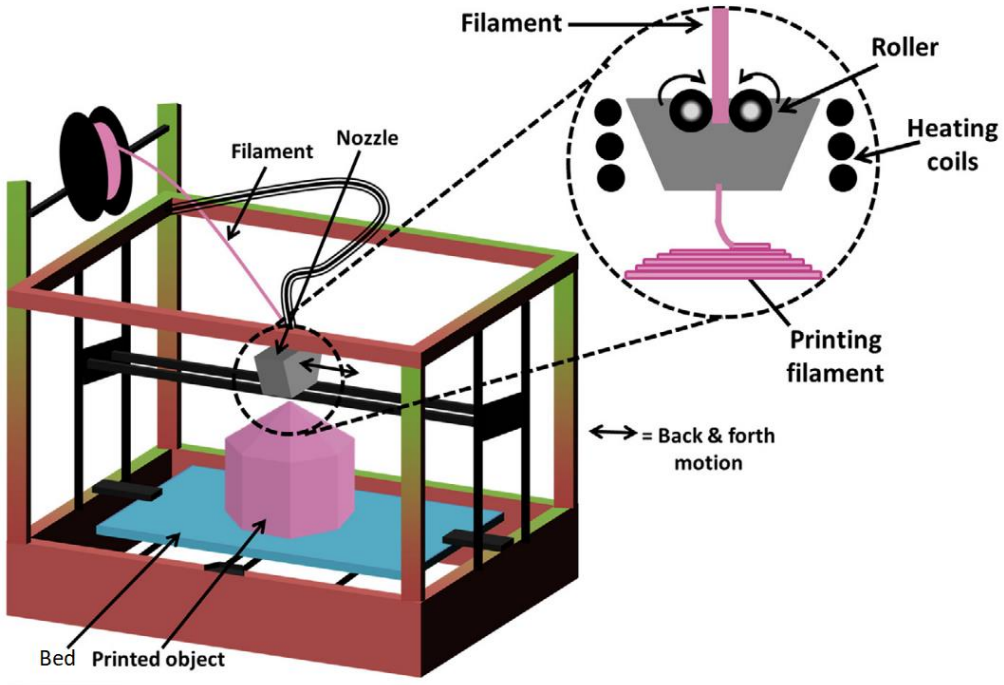

Figure 1.1. Illustration of the FDM set-up (adapted from [33]).

1.2. Materials

AM requires specific materials in order to print parts and components which will suit their applications. For certain AM processes, there are specific materials from each class that can be used for that process, but there are others which can be used in more than one method.

1.2.1. Metals

Metal alloys such an Ti alloys, Ni-based superalloys, Al alloys and steels have been successfully used in manufacturing through AM processes [34]. Steels account for almost a third of all metals made through AM processes, even though they are still mainly fabricated through conventional processes, such as casting and machining [35]. Since steel is a 100%

recyclable material, AM can add advantages in the circular economy, through the production of high added-value products from recycled powders and the enabling of the reuse of AM by-products in new products [36]. Powder bed fusion processes are the most used methods for the AM processing of metals [37]–[40]. Through this method, it is possible to reuse powder which has not been melted or sintered, in every swipe. Oxygen content between particles increases with every cycle, which in turn increases the oxidation of the powder content, which may lead to the manufacture of improper parts and components. This leads to the powder being unfit for reusability. Once it cannot be reused, it has to be discarded. This can have a negative impact for the environment [41]. This process may pose health hazards as well, through the formation of hazardous gas when processing, if the protective atmosphere is not properly calibrated [42]. Exposition to hazardous metallic particles can occur through many of the steps required to produce parts through this method, which poses a health risk as well, if not properly handled [43]. It also requires a higher output of energy, due to the utilization of laser and high-energy methods [44]

1.2.2. Ceramics

Due to the hardness and brittleness of finished ceramic parts, it is difficult to machine them without the introduction of defects and surface microcracks. Furthermore, the cost for such processes are high due to the use of diamond abrasives and cutting tools. These usually account for more than 70% of total manufacturing costs [45]. Because of this, ceramics are produced through dry powder sintering, or through the sintering of a ceramic powder paste mixed with bonding agents, or a ceramic suspension. For powder sintering, the two AM processes extensively used to manufacture parts are SLM and DED [46]–[48]. Both processes require high amounts of energy in order to process the material [44]. The sintering of ceramic paste is classified as a “multi-step” AM process. After the formation of the green body (ceramic body before sintering [49]), debinding and sintering thermal treatments are required in order to achieve the desired final part [48]. Through Inkjet printing it is also possible to manufacture ceramic parts [50]–[52].

1.2.3. Polymers

Polymers are a class of materials which are characterized for their high elastic and plastic properties. They are categorized as elastomers, fibres, thermoplastics and thermosetting.

Thermoplastics are a class of amorphous or semi-crystalline polymers that soften when heated above their glass transition temperature (T_g) and behave like a fluid. This process is completely reversible, as there are no bonding alterations at a chemical level [53]. Thermoplastics have been widely used in FDM, thanks to its' ability to produce parts and components with a complex geometry, in small environments, such as an office. In FDM processing, the spool of plastic filament feeds a heated nozzle. Afterwards, it is mechanically extruded as a thin wire with the desired diameter as specified by the nozzle [13], [53]. After being extruded, the polymers' temperature drops, and its' viscosity increases, which allows it to retain the desired shape [53].

To properly manufacture parts via FDM with these materials, there are properties which must be taken in consideration. For example, the thermoplastic viscosity has to be appropriate for the printer head to extrude and form a continuous stream of filament to ensure geometrical fidelity, rapid viscosity recovery after extrusion, in order to retain the desired shape for that layer and sufficient mechanical strength after being deposited on the printing bed of subjacent layer. This is required in order to support the following printed layers, as well as to prevent delamination (lack of adhesion between layers), during and after printing[53], [54]. The thermoplastic materials should exhibit a shear-thinning behaviour as well [53], [55]. Amorphous thermoplastics should be used since their solidification occurs at a faster rate, with less degree of shrinkage [56].

This section will present the polymeric materials which will be studied in this master dissertation. The materials which will be studied are neat Thermoplastic Polyurethane (TPU), Acrylonitrile Butadiene Styrene (ABS), Poly(Methyl Methacrylate) (PMMA) and High Impact Polystyrene (HIPS).

1.2.3.1. Thermoplastic Polyurethane

TPU is a copolymer with soft and hard segments which form a two-phase microstructure [57]. It has a low T_g and is suitable for FDM processing. However, there are some challenges

regarding the printing, due to the high viscosity and low Elastic Modulus (*E*) of it, which promotes filament buckling in the nozzle [56], [58]. Still, it is utilized due to the high abrasive and chemical resistance, and low price [59]. Through appropriate processing conditions, TPU can exhibit shape memory properties. For this effect to occur, the recommended temperature for extrusion is the range of 185 and 190ºC, in order to extrude a good quality shape memory sample [60]. After the part is printed, heating it to a value above T_g, shaping it to a different geometry and lowering the temperature below T_g while holding that shape will make it retain the transformed geometry, until it is heated above T_g again [61]. This phenomenon expands the use of this material, and the areas in which it can be applied. TPU has mechanical properties that of a rubber, but it can be processed as a thermoplastic [62]. Xiao et al. [63] state that different printing temperatures promote different mechanical properties. For an extrusion temperature of 215 ºC and an orientation angle of 45º for printing, its tensile strength and elongation at break had the highest values (46.2 MPa and 702%, respectively), which makes these the optimal parameters for printing TPU. For an extrusion temperature of 230ºC, the values obtained were inferior, but still higher to those of specimens printed at 200 ºC extrusion temperature. It was reported by de León et al. [64] that the extrusion of TPU filament from a temperature of 250 ºC caused degradation of the material, with the extruded filament turning black.

1.2.3.2. Acrylonitrile Butadiene Styrene

ABS is a copolymer composed by acrylonitrile-, butadiene- and styrene-containing monomers [65]. It is an amorphous thermoplastic with high impact resistance, high heat resistance, toughness, and low thermal conductivity. It can be classified into two types: moulding and another for printing [66], [67]. Fernandez-Vicente et al. [68] studied the printing of ABS and tested various parameters, including material density and infill pattern. The parameters that provide the highest tensile strength were the linear pattern with a 100% infill density. Markiz et al. [69] tested different printing directions for ABS specimens. They concluded that 0º printing direction increased strength of the specimens by 44.7%. It was also concluded that printing direction has no effect on the elastic modulus of the tested specimen. Cress et al. [70] tested the effect of multiple-stage recycled ABS on the mechanical behaviour and structure of printed specimens. It was found that recycled ABS

specimens had inferior performance when compared to virgin specimens. Nevertheless, the recycling process had little impact on the filament tensile strength, which indicates that the poor mechanical properties of the printed recycled specimens are due to cavities and porosity induced during the printing process. These results indicate that the printed parameters were not optimized for the specific recycled filament.

1.2.3.3. Poly(methyl Methacrylate)

PMMA is a clear, lightweight amorphous thermoplastic with high optical transparency, high scratch and impact resistance, favourable processing qualities and biocompatible properties [71]–[73]. It is referred to as Acrylic Glass. It is an alloplastic which can be used in biomedical applications, such as bone grafting [74]. Espalin et al. [75] reported that the extrusion temperature of 235 ºC provided the best raster surfaces with minimal material residue, while a higher temperature of 270 ºC created rasters with visible wavy surfaces and left material residue, which affected the part's geometry. An extrusion temperature of 225ºC created extremely stiff rasters which had low adhesion to a support material. It was also stated that transverse orientation printed specimens yielded mechanical properties which were more desirable, such as a higher value for compressive strength and modulus, when compared to axial orientation printed specimens.

1.2.3.4. High Impact Polystyrene

HIPS is a low-cost heterophasic thermoplastic which has a high processability, and presents high impact strength and low tensile strength [76], [77]. It is obtained from the radical polymerization of an homogenous solution containing polystyrene and polybutadiene (PB) copolymer [78]. Kaveh et-al.[79] analysed three printing temperatures, in order to cover the recommended range of extrusion and to obtain the optimal extrusion temperature. For the studied temperatures of 210, 220 and 230 ºC, an extrusion temperature of 210 ºC was selected as the optimal temperature, as a temperature of 220 ºC showed reduced precision in the print, and a temperature of 230 ºC promoted the appearance of internal cavities (air bubbles in the filament).

1.3. Multi-material 3D Printing

In recent years, multi-material polymer parts manufacturing through FDM has caught the attention of both the industry and academic community [77]. With multi-material FDM, it is possible to enhance the mechanical properties, improve printing performance and enable new functionalities for the printed parts and components [80]. Through different arrangements and combinations of polymers, it is possible to achieve said objectives for customized products [81]. Multi-material 3D printing can be applied to 4D structures to provide specific shapes, properties and functionalities [82]. It is also possible to print with multiple colours – multi-colour FDM. While not engaging in any of the advantages of multi-material FDM, since the filaments used are composed from the same material with different colours, it is a viable low-cost process to create visual models and parts where it is important to emphasize different sections or areas in them [83]. The applications for these are not the same for multi-material FDM.

1.3.1. Sandwich structure

Usually, sandwich structured composites include a lighter and softer core material, with the outer portions (skins) being printed in a higher-strength material [84]. Figure 1.2 shows an example of a printed sandwich structure multi-material specimen.

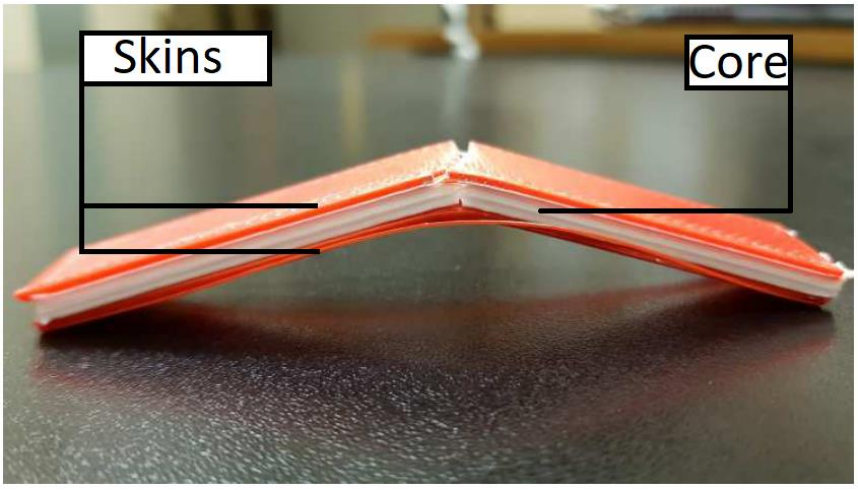

Figure 1.2. Example of a printed sandwich structure multi-material specimen (adapted from [88]).

The core can provide the part or component with flexural stiffness, out-of-plane shear and compressive strength, while the outer portions (skins) bear most of the bending and in-plane loads that take place. The performance of the structure depends on the properties of the skins and the core, the adhesion between them and the geometry of the final part [85]. The printing parameters must be optimized in order to promote the maximal adhesion between the different materials. These parameters have a great influence on the mechanical properties of the final part as well. To maximize the value for Young's Modulus and stiffness, the printed layers should be oriented along the loading line, and in order to promote the best performance in strength, stiffness and ductility, the building orientation should be on-edge [86], [87]. Lopez et al. [77] evaluated the tensile properties of different material combinations of sandwich structures produced through FDM. The materials which were tested were: PLA (Polylactic Acid), ABS and HIPS, in different combinations. It was found that the combination which showed the best testing result was the combination of ABS core and PLA skins. It was concluded that sandwich structures applied to 3D printing can bring out the properties of two different materials in the same produced part. Singh et al. [76] evaluated the tensile properties of specimens composed of different combinations of PLA, HIPS and ABS. It was observed that, while HIPS had the lowest peak strength of all materials tested, when printed as a multi-material specimen with equal parts of PLA and ABS there was an improvement in the tensile strength (from 27.4 kg/m^2 to 28.81 kg/m^2). It was found that multi-material printing through FDM of various thermoplastics is possible and can lead to the improvement of the mechanical properties of printed parts. Brischetto et al. [88] studied the mechanical behaviour of polymeric sandwich specimens with honeycomb cores. For this study, specimens were fully printed with a single material, with different printing patterns for distinct parts of the specimen, and multi-material printer, with distinct materials for the core and skins. Specimens were printed with PLA and ABS. The skins were printed using a linear pattern, while the core of the specimen was printed either with a honeycomb infill configuration or a linear infill configuration. When utilizing two different extruders to print a PLA core with hexagonal infill and ABS skins, lower performances for the elastic modulus were observed. This happened due to bad adherence between the skins and the core, because of the materials used (ABS, PLA) and the utilization of two extruders to print the subsequent three layers. This effect was minorized through the alteration of the PLA core, through the use of a homogenous 100% linear infill PLA core in

place of the hexagonal infill PLA core, when ABS skins are utilized, to promote a greater adhesion between the different materials. It was suggested that the transition between the first and second extruder allowed for the previously printed layer to have an early cooling, which compromised the adherence of the following layer.

In this work, TPU will be used as the core of the specimens, while ABS, HIPS, and PMMA will be used as skins.

1.4. Mouthguard Production through 3D Printing

Previous works have been done to study the possibility of producing mouthguards for athletes through FDM with materials other than EVA. This approach would enable the production of fully customizable devices while guaranteeing the comfort of the wearer through the reduction of the device's thickness to 2 mm.

A previous work [89] concluded that to promote comfort for the wearer while guaranteeing the best mechanical properties for the mouthguard, multi-material printing might be the answer. This work continues that study through the mechanical testing of mono-material and multi-material specimens, non-aged and that have been aged in an artificial saliva solution, as suggested.

2. EXPERIMENTAL PROCEDURE

2.1. Materials

In the present work, different polymeric materials were utilized and studied. The materials were commercially purchased and used without further modifications: Acrylonitrile Butadiene Styrene and High Impact Polystyrene provided by DoWire®, Seixal, Portugal; Thermoplastic Polyurethane and Poly (Methyl Methacrylate) provided by TreeD Filaments™, Seregno, Italy. The filaments presented a diameter of 1.75±0.03 mm.

The characterization of the filaments was made, presented, and discussed in previous works.

The filaments were chemically characterized by Fourier Transform Infrared Spectroscopy (FTIR), Thermogravimetric Analysis (TGA) and Differential Scanning Calorimetry (DSC) were used for the thermal characterization. The mechanical properties were determined by Tensile Testing. FTIR identifies functional chemical groups of polymeric materials [90]. TGA analyses the thermal stability of a material by evaluating the variation of mass with temperature [91]. Differential Scanning Calorimetry determines the heat flux difference between the material and a reference material, during a controlled temperature program with pre-defined heating and cooling rates. From the obtained results it is possible to determine the thermal events of the polymeric filaments [91]. Tensile testing subjects a sample with an increased controlled load, in order to observe the capacity of the material to resist to the imposed solicitation [92].

2.2. Processing by 3D Printing

All the printed specimens were processed in a FlashForge^{TM} Creator 3 3D printer with a dual extruder system, each one is coupled with a single nozzle with a diameter 0.4 mm.

The printing parameters for each material are presented on Table 2.1. A layer height of 0.18 mm was kept constant for all the printed specimens. 100% LIN specimens were printed with an orientation angle of $+45^{o}/-45^{o}$.

Table 2.1. Printing parameters for the different studied specimens.

Material	Infill Pattern	Printing Temp (ºC)	Bed Temp (ºC)	Speed (mm/s)
ABS	15% 3D	220	110	50
	15% HEX			
	100% LIN			
HIPS	15% 3D	220	110	50
	15% HEX			
	100% LIN			
PMMA	15% 3D	220	110	50
	15% HEX			
	100% LIN			
TPU	100% LIN	220	110	15
ABS-TPU	100% LIN	220	110	15
HIPS-TPU	100% LIN	220	110	15
PMMA-TPU	100% LIN	220	110	15

2.3. Characterization of specimens after printing

All the characterization tests were performed in order to have at least 5 valid tests for each type of printed sample. Considering that the characterizations were made before and after the aging process in artificial saliva, the next sub-section describes the aging procedure.

2.3.1. Aging test in artificial saliva

Artificial aging is a process in which a specimen is put into a specific environment with controlled conditions, for a determined period of time, in order to assess the impact of such environment on the properties. In the present wok, the effect of the aging test was evaluated in the mechanical properties [93].

In the aging process, the printed specimens were stored inside individual Falcon® Graduated tubes which contained 12 mL of artificial saliva solution. The chemical composition of this solution is: 800 mL of distilled water (H_2O), 0.426 g of di-sodium hydrogen phosphate (Na_2HPO_4), 1.68 g of sodium bicarbonate ($NaHCO_3$), 0.147 g of calcium chloride ($CaCl_2$) and 2.5 mL of hydrochloric acid, 1M.

The Falcon® tubes were left inside a ThermoShaker (Incubator Shaker THO 500/1 from Gerhardt) for 14 days, at a constant temperature of 37ºC and 100 rotations per minute (rpm), to make sure every surface of the printed specimens would be in contact with the solution.

The 14 days are equivalent to the number of hours that an athlete will use the mouthguard for 1 hour per day during a period of one year (336 hours), and the 37ºC is the average human body temperature.

2.3.2. Three-point Bending test

The 3PB test starts with the setting of the appropriate span between the supports where the specimen to test will be placed on. In this work the span was determined through the application of the standard ASTM D790 [94], considering the thickness of the printed specimens, as represented on Figure 2.1.

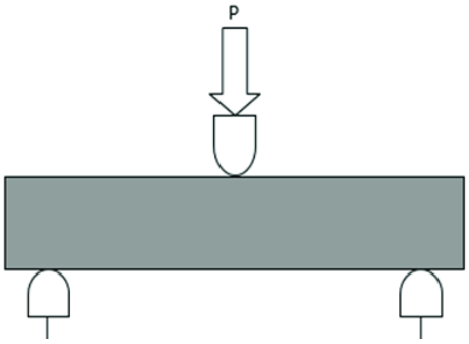

Figure 2.1. Three-point bending test, according to ASTM D790 (adapted from [114]).

The specimen is deformed through an applied load (P) until the maximum load is reached, or until fracture occurs [95]. The results are given as a load/displacement curve. It is possible to calculate the bending stress (σ) for a specific displacement or the maximum bending stress (σ_{MAX}) for the tested specimen, as well as the bending elastic modulus (E) of the material [96].

Figure 2.2 presents the geometry and dimensions of the printed specimens according to standard ASTM D790 [94].

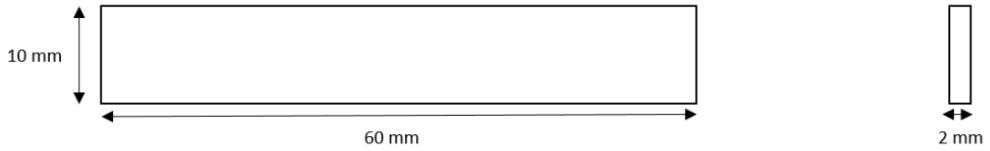

Figure 2.2. Geometry of printed specimens for 3PB testing, according to the standard ASTM D790. (adapted from [89])**.**

Table A.1 of Appendix A presents the mean dimensions for printed specimens for 3PB testing.

The testing equipment which was used was a Shimadzu model Autograph AGS-X, with a 5 kN load cell and a displacement rate of 2 mm/minute. The results obtained were collected by the software Trapezium X.

2.3.3. Transverse Impact test

The Transverse Impact test or Charpy test is a destructive test which allows the determination of the resistance of a material to an impact [97]. When the pendulum is released from its support, which is at a pre-determined height, it transfers the kinetic energy to the specimens. These are placed on two lateral supports, properly centred, allowing the pendulum to hit the geometric centre of the sample [98]. A transverse impact testing equipment with a Charpy pendulum is represented in Figure 2.3.

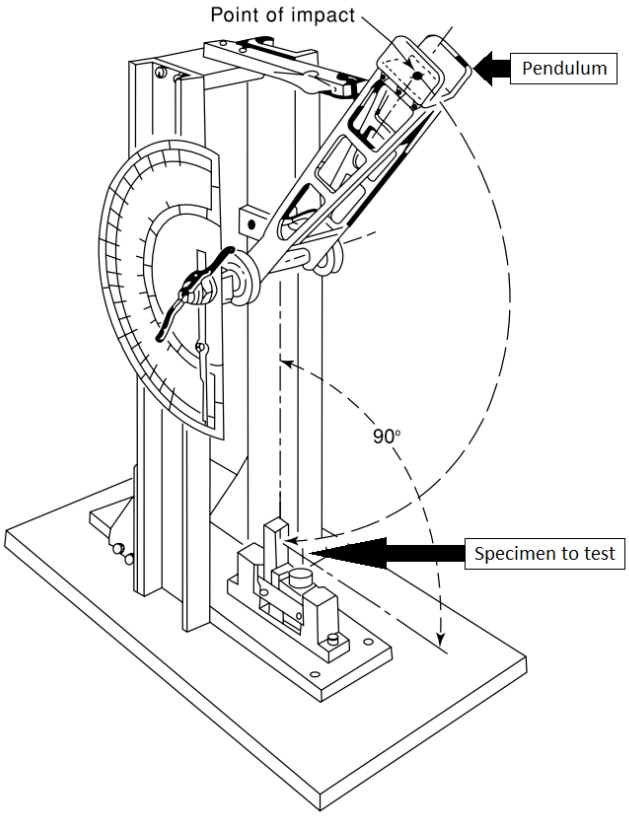

Figure 2.3. Transverse impact testing equipment with a Charpy pendulum (adapted from [98]).

The test measures the resilience of the material and the amount of energy absorbed during impact [99]. Resilience is commonly defined as the capacity of the material to absorb the energy and is calculated through the total energy transferred and the area of the section of the tested specimen [100]. The absorbed energy is measured in the percentage of the total energy and is determined as the difference between total impact energy applied by the pendulum and the dissipated energy. As expected, the lower the dissipated energy, the higher the absorbed energy on the impact zone, which in turn will amplify the negative effect on the structural integrity of the tested sample [99].

Specimens were printed with the dimensions according to the standard Charpy ISO 179 [101], with 80 mm in length and 10 mm width, as well as 2 mm thickness. A notch in the shape of a "V" was also included in the geometry of every tested specimen, as shown in Figure 2.4. Table A.2 in Appendix A presents the mean values for the dimensions of these specimens.

The tests were performed in an Instron Ceast 9050 equipment, with an impact pendulum of 5 J, positioned at an angle of 150º.

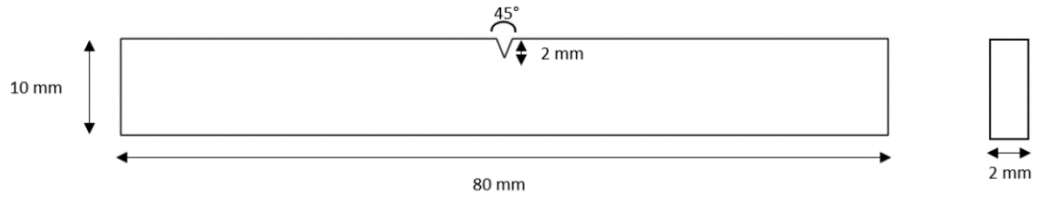

Figure 2.4. Geometry and dimensions of the specimens for the transverse impact test, according to the standard Charpy ISO179 (adapted from [89]).

2.3.4. Macroscopic Analysis

To evaluate the morphology of the damage which had been done on every type of printed specimen subject to the impact tests, a macroscopic analysis was made. The evaluation used Carl ZEISS model Stemi 2000-c equipment, with a magnification factor of 5 times. A digital camera CANON, model POWERSHOT G5, with a magnification factor of up to 16 times was used for the macrographs acquisition.

3. ANALYSIS AND DISCUSSION OF RESULTS

3.1. Results from previous works

As previously stated, this work continues the previous studies which have been made into the production of mouthguards through means of FDM. As so, the filaments used to produce the specimens which were tested in this work were characterized by previous authors.

Previous MSc students characterized the HIPS, PMMA and TPU filaments [89] as well as the ABS filament [102]. They have concluded, through FTIR characterization, that the presence of additives on the filament did not influence the global chemical composition of each polymeric material. The TGA evaluation showed that all filaments were thermally stable up to a temperature of 332ºC. The DSC results indicated that all filaments were amorphous, and the respective T_g values are listed in Table 3.1.

Table 3.1. Values for glass-transition temperatures obtained from previous works.

Filament	T_g(ºC)
ABS	110.7
HIPS	99.0
PMMA	113.5
TPU	-21.4 66.9

TPU presented two T_g values. This fact is consequence of TPU being composed of soft segments of poliol-diisocyanate in long chains and hard segments formed in the borders between diisocyanates and small chains of polyol [59].

3.2. Saliva-induced aging

The dimensions of the specimens were measured before and after the ageing tests. This was done in order to understand if the geometry of the printed specimens would change with the moist environment during use, indicating the absorption of saliva. The variation of the dimensions of the printed specimens could jeopardize the efforts of producing a mouthguard that would be the most comfortable for the athlete, as well as compromise the retention of the device.

Both mono and sandwich structure printed specimens were measured before and after the aging process. Table 3.2 shows the dimensions and variation in the specimens for the 3PB test. Table 3.3 lists the results for the specimens printed for the impact test.

The obtained results show no significant variation of the dimensions due to the immersion in artificial saliva.

This confirms that all thermoplastic used in this work are hydrophobic, as expected [89], [103]–[106]. This is an important factor to take in consideration since the accumulation of saliva on the mouthguard could also lead to the proliferation of bacteria onto the device.

Table 3.2. Mean average and standard deviation values of the dimensions of the printed specimens for the 3PB tests, before and after the aging process.

Material	Infill	Length (mm)		Width (mm)		Depth (mm)	
		Before	After	Before	After	Before	After
ABS	15% 3D	59.7*	59.7*	9.9*	9.9*	2.2*	2.1*
	15% HEX	59.8*	59.7*	9.9*	9.9*	2.2*	2.1*
	100% LIN	59.8*	59.9*	10.0*	10.0*	2.1*	2.1*
HIPS	15% 3D	59.7 ± 0.1	59.6 ± 0.1	9.9*	9.9*	2.1*	2.1*
	15% HEX	59.7*	59.6*	9.9 ± 0.1	9.9*	2.0*	2.0*
	100% LIN	59.8*	59.7 ± 0.1	9.8 ± 0.4	10.0*	2.1*	2.1*
PMMA	15% 3D	59.8*	60.0 ± 0.1	10.0*	10.0*	2.1*	2.1*
	15% HEX	59.7*	59.9*	10.0*	10.0*	2.1*	2.1*
	100% LIN	59.9*	60.2 ± 0.1	10.2*	10.2*	2.1*	2.1*
TPU	100% LIN	59.9 ± 0.2	60.2 ± 0.1	10.4 ± 0.2	10.4 ± 0.2	2.1 ± 0.2	2.1 ± 0.2
ABS-TPU	100% LIN	60.3 ± 0.1	60.3 ±0.1	10.4 ± 0.1	10.4 ± 0.1	2.4 ± 0.1	2.4 ± 0.1
HIPS-TPU	100% LIN	60.3 ± 0.1	60.2 ± 0.1	10.4 ± 0.1	10.3 ± 0.1	2.3*	2.4*
PMMA-TPU	100% LIN	60.1 ± 0.1	60.3 ± 0.1	10.4 ± 0.1	10.4 ± 0.1	2.5*	2.5*

*Values with standard deviation of 0.0

Table 3.3. Mean average and standard deviation values of the dimensions of the printed specimens for the impact tests, before and after the ageing process.

Material	Infill	Length (mm)		Width (mm)		Depth (mm)	
		Before	After	Before	After	Before	After
ABS	15% 3D	79.5 ± 0.1	79.8*	9.9*	9.9*	2.1*	2.1*
	15% HEX	79.5*	79.6*	9.8*	9.9*	2.0*	2.0*
	100% LIN	79.5 ± 0.1	79.6 ± 0.1	9.9*	9.9*	2.1*	2.1*
HIPS	15% 3D	79.5 ± 0.1	79.4*	9.9 ± 0.1	9.9*	2.0*	2.0*
	15% HEX	79.5*	79.4*	9.9*	9.9*	2.1*	2.1*
	100% LIN	79.6 ± 0.1	79.5*	9.9*	9.9*	2.1*	2.1*
PMMA	15% 3D	79.6 ± 0.1	79.8*	10.0*	10.0*	2.1*	2.1*
	15% HEX	79.6*	79.8*	10.0*	10.0*	2.1*	2.1*
	100% LIN	79.8 ± 0.1	80.0 ± 0.1	10.1 ± 0.1	10.1 ± 0.1	2.1*	2.1*
TPU	100% LIN	80.2 ± 0.1	80.3 ± 0.1	10.5 ± 0.3	10.6 ± 0.1	2.1 ± 0.1	2.2 ± 0.2
ABS-TPU	100% LIN	84.0 ± 0.1	84.1*	10.7*	10.8*	2.4*	2.4*
HIPS-TPU	100% LIN	84.0 ± 0.1	84.0 ± 0.1	10.8*	10.8*	2.4*	2.4*
PMMA-TPU	100% LIN	84.1 ± 0.1	84.3 ± 0.2	10.9 ± 0.1	10.9 ± 0.1	2.5*	2.5*

*Values with standard deviation of 0.0

3.3. Mechanical Properties of Mono-materials

3.3.1. Three-point bending test

Three-point Bending testing was done, in order to determine the maximum value for the bending stress (σ), as well as the bending elastic modulus (E). As previously stated, different materials and patterns for the infill were tested, to characterize them as printed and after the ageing test, but also to have the knowledge of the behaviour of each material in order to understand results of the sandwich structures.

Specimens which were aged in saliva were kept inside the aging solution and removed from it right before testing, to ensure they would stay soaked in artificial saliva until testing. Cumings et al. [107] states that the rigidity of the material is a property to consider when manufacturing mouthguards, since a material which is more rigid (higher value for E) has a higher probability to distribute resulting stress from impact and, as a consequence, reduce stress applied to the tooth-bone interface.

The maximum value for the bending stress (σ) in the transverse section was obtained through the maximum load value (P), the specimen's thickness (h) and width (b), and the span between the supports in which the specimen would be laid to (L), according to Equation (1) [94].

$$\boldsymbol{\sigma = \frac{3 \cdot P \cdot L}{2 \cdot b \cdot h^2}} \quad (1)$$

Figure 3.1 shows the stress-displacement curves for ABS, HIPS and PMMA, with different infill patterns and aging situations, for a span of 40 mm.

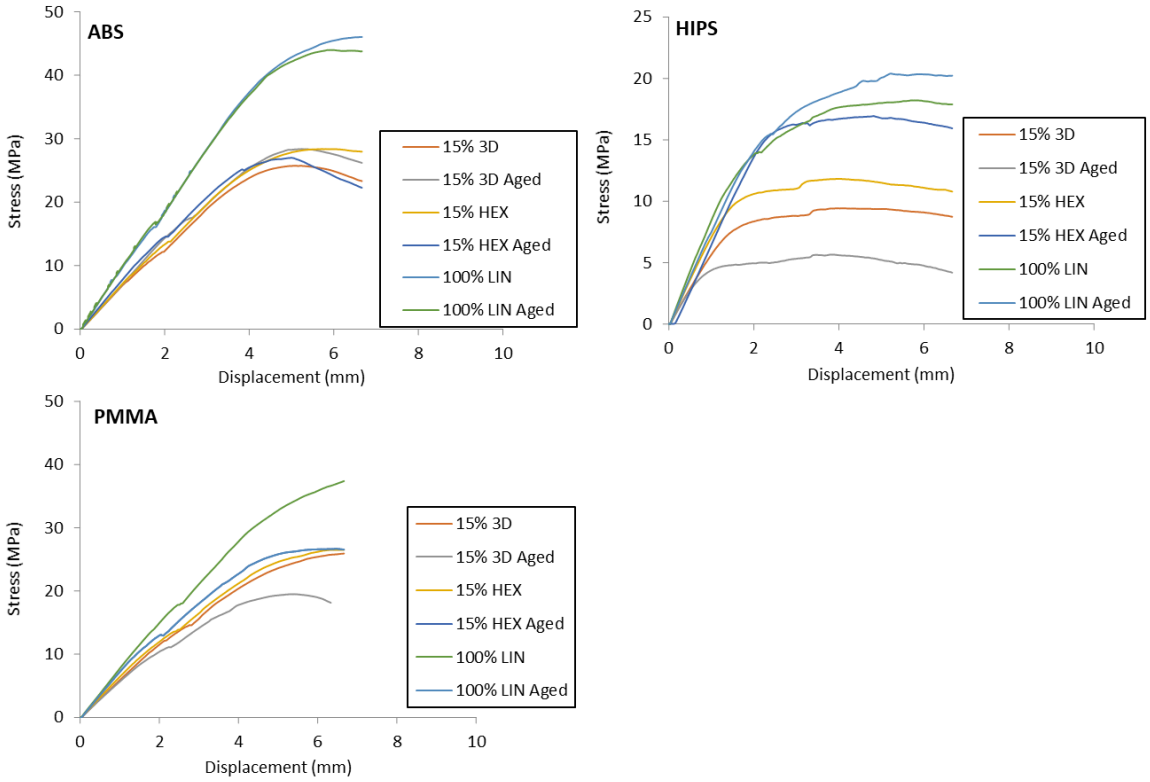

Figure 3.1. Stress-displacement representative curves for the printed mono-material specimens.

The bending elastic modulus (E) was obtained through the slope of the initial part of the stress-displacement curve. It was obtained from the load interval in the linear segment of the stress-displacement curve (ΔP), the displacement in the linear segment of the curve ($\Delta \mu$) and the moment of inertia of the specimen (I), according to Equation (2) [94].

$$E = \frac{\Delta P \cdot L^3}{48 \cdot \Delta \mu \cdot I} \quad (2)$$

The values for σ and E were determined, both for every material and configuration, and the results are presented in Figure 3.2 and Figure 3.3, respectively.

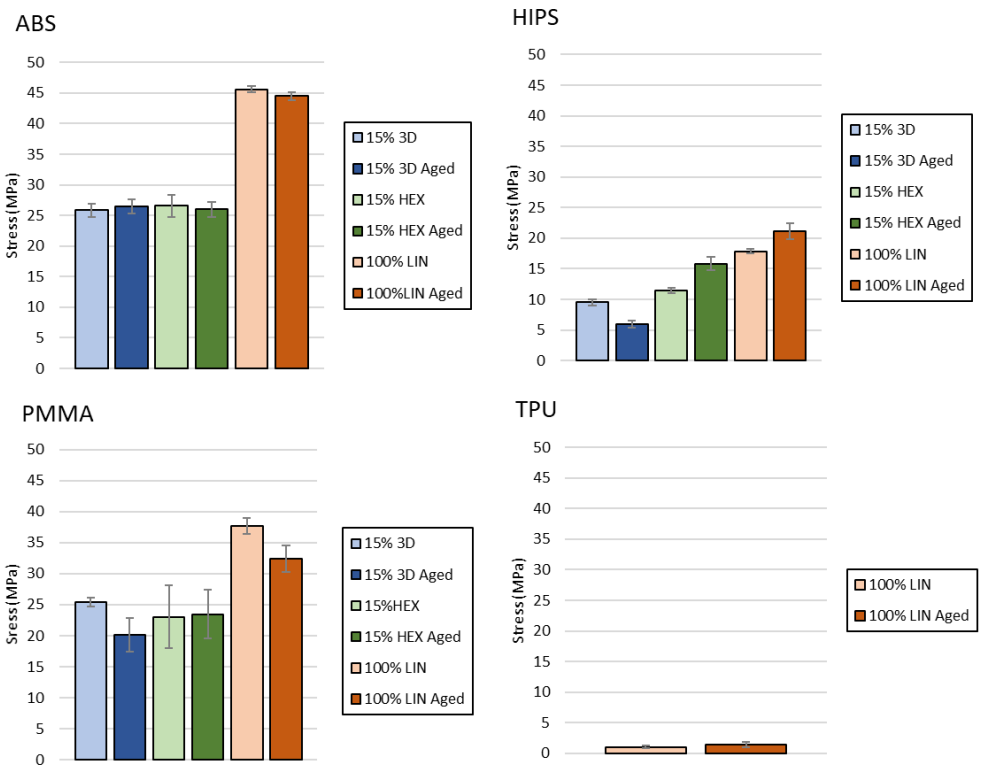

Figure 3.2. Maximum bending stress values of the mono-material printed specimens. Values are presented as mean ± standard deviation.

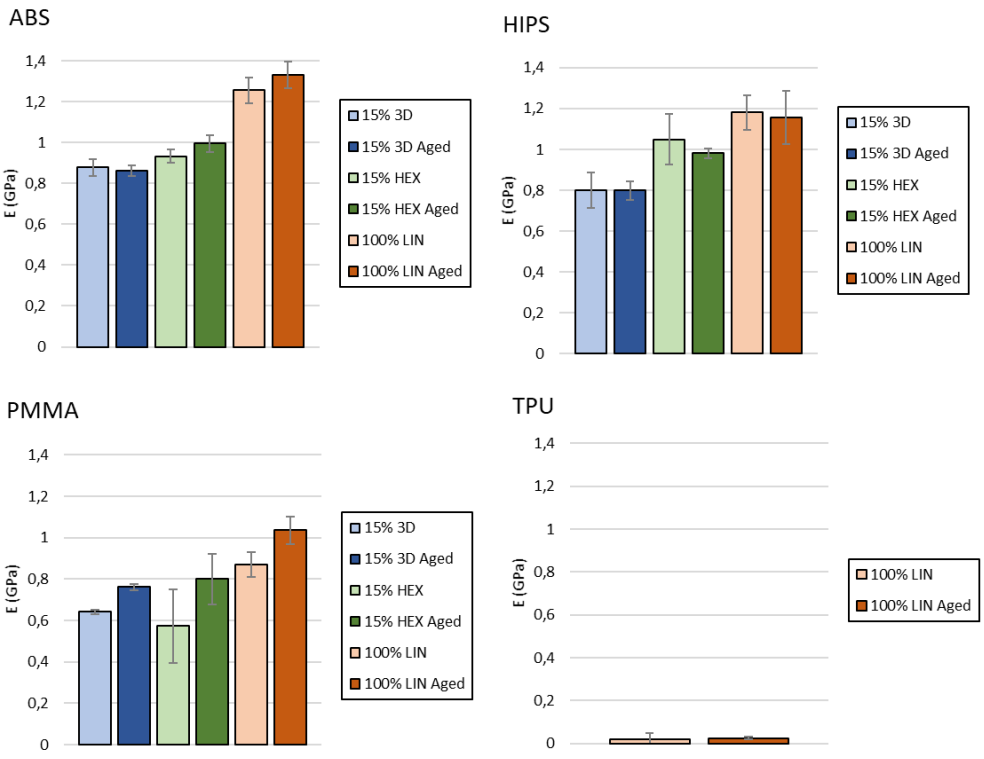

Figure 3.3. Bending elastic modulus of the mono-material printed specimens. Values are presented as mean ± standard deviation.

Overall, considering all the tested materials, it can be stated that the 100% linear infill pattern presents the best mechanical properties, either when tested as printed or after the ageing tests.

Considering the results from each material, ABS specimens with 100% linear infill pattern presented the highest values of σ and E. This pattern allowed the samples to deform plastically, with no fracture at the macroscopic scale, while most of the specimens printed with 15% 3D infill pattern and 15% hexagonal pattern fractured and delaminated in the outer layers. The process of ageing in artificial saliva had little or no impact on the mechanical behaviour of printed specimens.

PMMA printed specimens present lower values of σ than those of ABS, and the lowest values of E for all the tested specimens, independent from the infill pattern. 15% 3D and 15% hexagonal infill patterns promoted the fracture and delamination of the outer layers. Delamination was also observed in the specimens printed with a 100% linear infill pattern even though they did not present any fracture. The artificial saliva aging process had a higher impact on the mechanical behaviour of specimens printed with PMMA when compared to specimens printed in ABS. This fact is evident in the lower σ value and the increase in E (with the exception for 15% hexagonal infill pattern). This can be explained by the fact of the solution having different chemical compounds, which might have combined chemically with the polymeric chains from the specimens, originating new chemical chains. Even though the polymeric materials are hydrophobic, they can still absorb those chemical compounds present in the saliva solution, in areas in contact with it. It is most likely that the chemical absorption has occurred only in the outer layers of the printed specimens, which means that, globally, this reticulation was not enough to enhance the bending stress.

The specimens printed in HIPS presented the lowest values of σ, independently of the infill pattern. Still, the highest values for this material were observed in the specimens printed with 100% linear infill. Aging in artificial saliva had a positive impact on the maximum values for the bending stress, with the exception of specimens printed with a 15% 3D infill pattern, while the E values remained generally unchanged. Specimens printed with this polymeric material were the only that did not present fracture after plastic deformation, by the end of the test.

TPU specimens were printed after the testing of other specimens, hence only 100% linear infill pattern was tested. This was done in order to save time, as the process of printing

TPU requires lower speeds, and printing different infill patters would be unnecessarily time-consuming. In the previous work [89], non-aged TPU specimens with 100% linear infill pattern were characterized. The values for the maximum bending stress for printed TPU specimens were not possible to calculate and the presented values are the ones recorded at the end of the test. Still, it is possible to state that the elastic modulus for TPU specimens is the lowest, when compared to the other materials, as reported in the literature [108]. The aging process had no influence in the mechanical properties of specimens printed in TPU.

In Table B.1 of Appendix B it is possible to observe the mean values obtained for mono-material specimens by the 3PB tests.

3.3.2. Transverse Impact test

According to the standard ASTM F697-16 and ADA (American Dental Association), mouthguards must be manufactured with resilient materials, in order to minimize damage to the teeth and surrounding areas, especially in contact-heavy sports [109]–[112]. The capacity to absorb, dissipate and distribute energy during the physical activity must be optimized in order for the devices to fulfil their objectives [113].

The Transverse Impact tests were performed to evaluate the suitability of the studied materials for the presented requirements. Figure 3.4 indicates the mean average resilience values obtained through Transverse Impact testing and Figure 3.5 shows the mean average values for the absorbed energy.

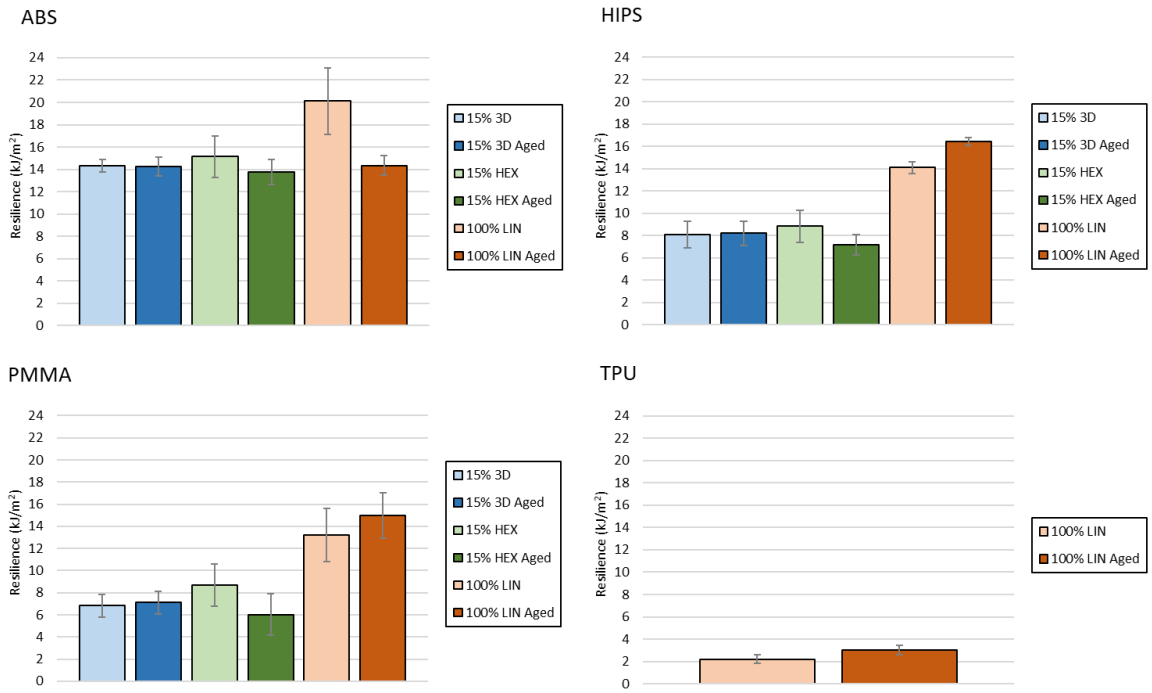

Figure 3.4. Resilience of the mono-material printed specimens. Values are presented as mean ± standard deviation.

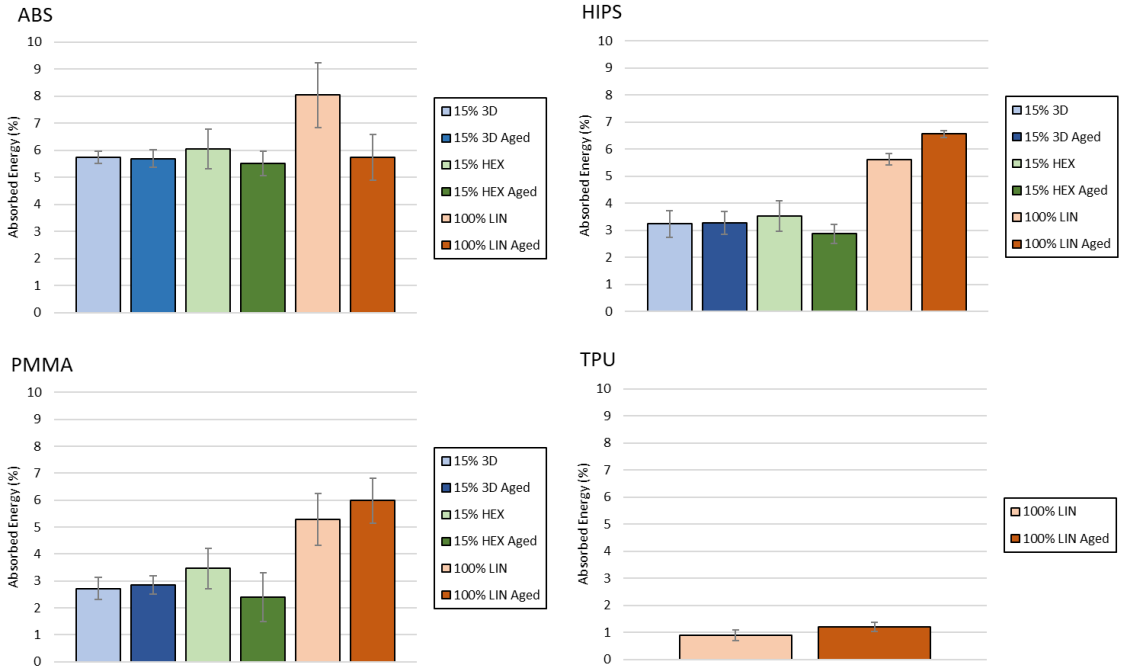

Figure 3.5. Mean average value of the absorbed energy for the printed mono-material. Values are presented as mean ± standard deviation.

The infill pattern which provides the specimens with the highest resilience values and the highest percentage of absorbed energy is the 100% linear pattern, while 15% hexagonal and 15% 3D infill patterns show practically similar results. These results can be explained due the amount of material used to produce these samples (100% against 15%). However, higher absorbed energy suggests that the dissipated energy will be lower, which might induce localized fractures (Appendix D).

Generally, it can be stated that the aging process in artificial saliva had no significant impact on the mechanical behaviour of the printed specimens other than that of 100% linear infill pattern ABS. For this material, the resilience for aged specimens decreased by 28.7%, and the energy absorbed by 34.4%, as a consequence of probable chemical reaction originating between the chemical compounds present in the solution and the polymeric chains of the printed specimen.

The partial conclusion of the characterization made for the printed mono-materials is that, except for the ABS, the aging process did not significantly change the mechanical properties of each material. For ABS, it seems that the artificial saliva solution acted as a plasticizer decreasing both σ and E values. However, in this case, the plasticizing effect must be mainly occurring only on the outer shell of the printed specimens, as all the materials are hydrophobic. This characteristic implies that the chemical compounds present in the saliva solution are not able to be absorbed by the polymer and therefore do not reach the inside of the printed material.

In Table C.1 of Appendix C it is possible to observe the mean values obtained from mono-material specimens by Transverse Impact tests.

Considering that the optimal set of properties should include high values of σ, E and resilience with low values of absorbed energy, the next step was to combine each one of the three materials with TPU.

3.4. Mechanical Properties of Multi-materials

Through multi-material printing it is possible to produce parts and devices from materials with different properties, which will result in printed specimens with different

properties. Lopez et al. [77] state that the type of material combination results in different properties being affected.

In this work, the printing configuration chosen to test was the sandwich configuration, in which TPU will be used as the core for every specimen, as schematically represented in figure 3.6. The overall thickness was 2mm and the 100% infill was chosen for all 3 layers of each printed specimen.

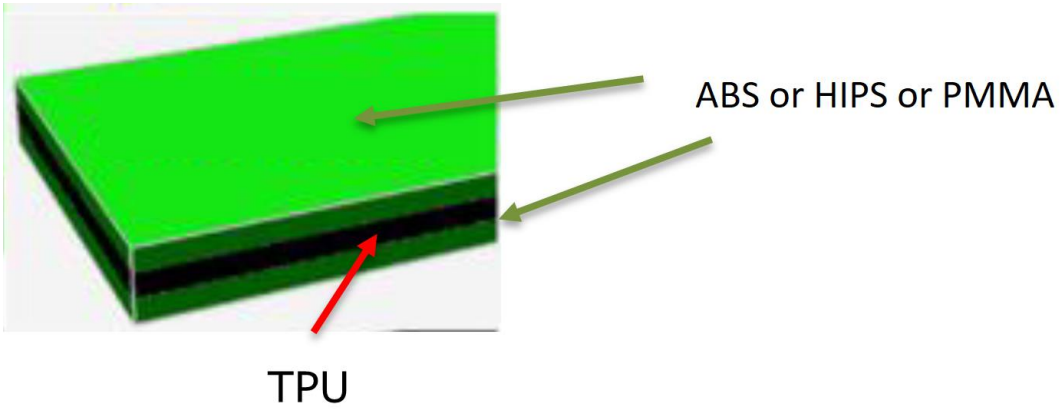

Figure 3.6. Schematic representation of the sandwich structures printed in multi-materials.

3.4.1. Three-point bending test

As for the 3PB tests for the mono materials, through the application of the Equations (1) and (2), it was possible to obtain the maximum value for σ and for E. Figure 3.7 shows the representative stress-displacement curves, for each printed sandwich specimen.

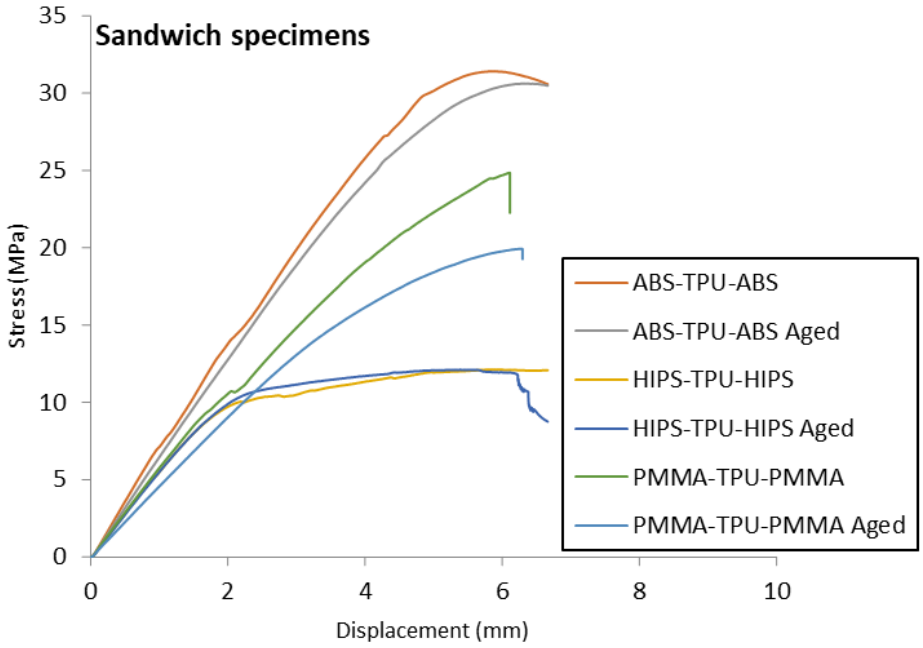

Figure 3.7. Stress-displacement representative curves for the printed sandwich specimens.

The results obtained from these tests are displayed Figure 3.8 for the maximum bending stress, and in Figure 3.9 for the elastic modulus.

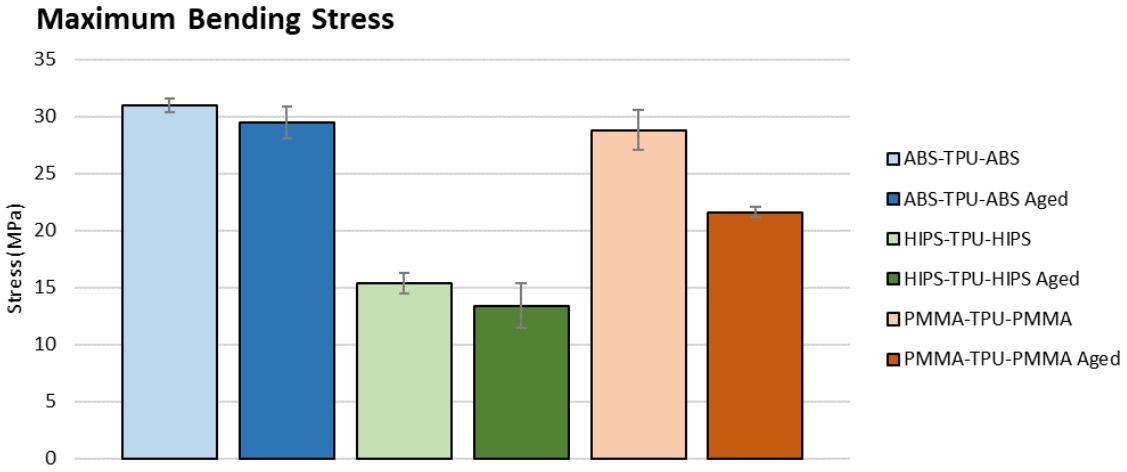

Figure 3.8. Maximum bending stress values for the printed sandwich specimens. Values are presented as mean ± standard deviation.

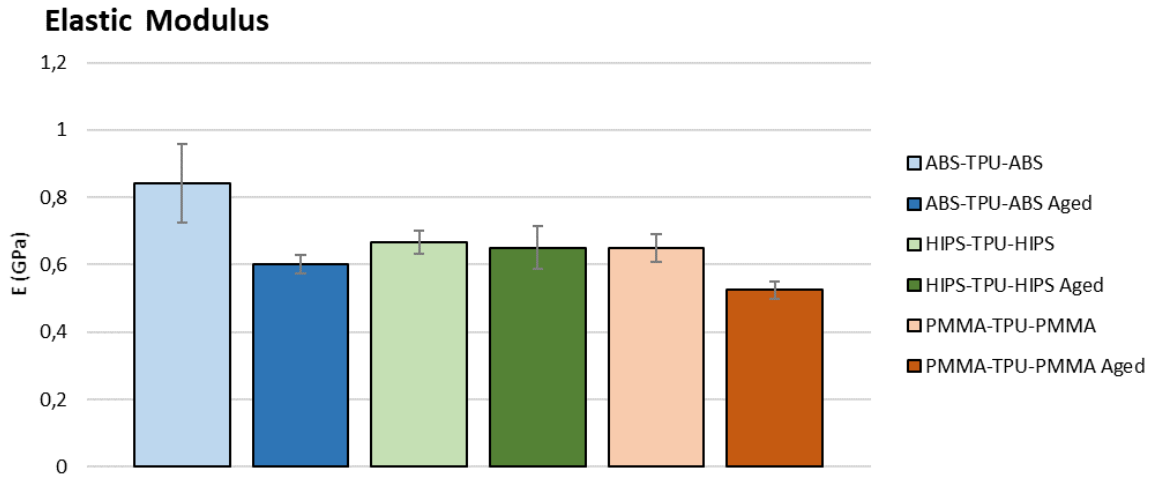

Figure 3.9. Bending elastic modulus for the printed sandwich specimens. Values presented as mean average ± standard deviation

The inclusion of TPU in the sandwich structures resulted in a decrease of the values of σ and E, for both the as printed and aged specimens and for all the tested materials. This is an expected result because 1/3 of the overall volume of the specimen is composed of TPU, a polymer with very low values for the tested mechanical properties. Moreover, as stated by Brischetto et al. [88], bad adhesion can be observed occasionally with some material combinations, which will have an impact in the results. In fact, during testing, the core and skins of some of the multi-materials were completely separated.

Nevertheless, it must be highlighted the fact that ageing tests presented no effect in the multi-material specimens, in opposition to what happened in the mono-material specimens. The reason can be due to the presence of TPU as well, which, as mono-material, showed a more homogeneous mechanical behaviour in the presence of the artificial saliva. These results are very important, as they indicate that the overall performance of the mouthguard will be maintained, independently of the number of times that the device is used by the athlete. Table B.1 of Appendix B presents the mean values obtained for multi-material specimens by the 3PB tests.

3.4.2. Transverse impact test

The resilience of each type of multi-material structure tested is presented in Figure 3.10 and Figure 3.11 shows the absorbed energy values for the same specimens.

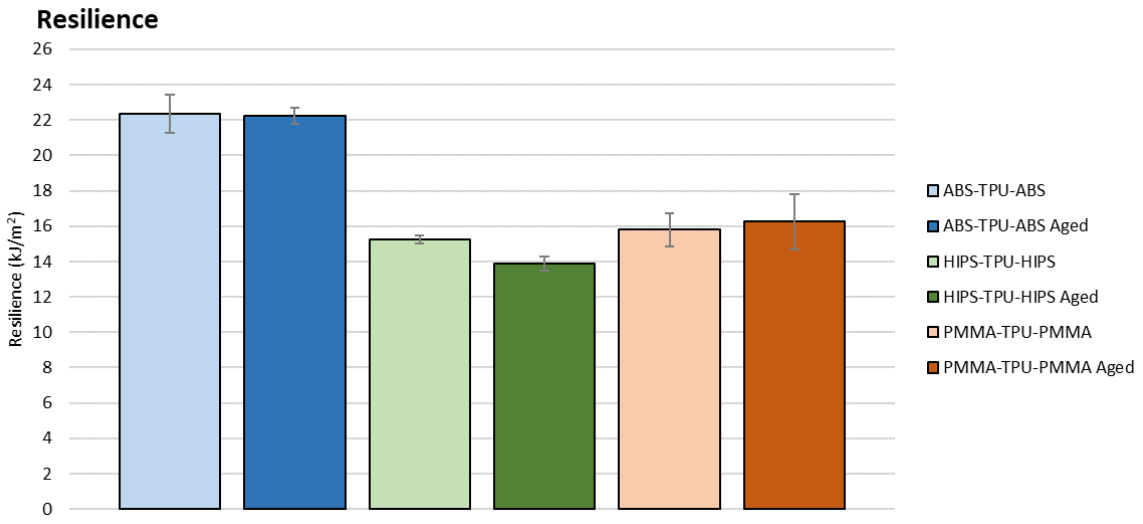

Figure 3.10. Mean average value of the resilience for the multi-material sandwich structures. Values are presented as mean ± standard deviation.

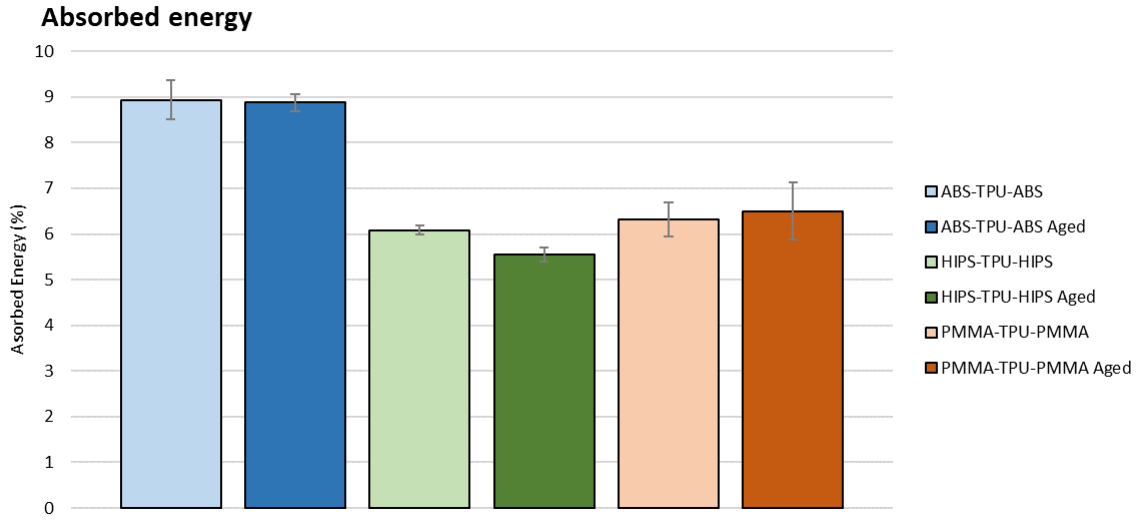

Figure 3.11. Mean average value of the absorbed energy for the printed multi-material sandwich structures. Values are presented as mean ± standard deviation.

The inclusion of TPU in the multi-material sandwich structures resulted, overall, in a stabilization of the values observed before and after the ageing process, for all materials, which is a very significant result as explained before.

Considering the standard deviations (maximum and minimal values) of the obtained results of the resilience and absorbed energy it can be observed that no significant differences exist between the mono and multi-materials, with a tendency for a slight increase in the evaluated properties for multi-material specimens.

The only exception that is worth mentioning is the ABS-TPU-ABS sandwich structure. In this case a more significant increase in the mean values was observed. In fact, the increase of the resilience and absorbed energy of the tested specimens after the ageing process increased by 11% when compared to the results of the mono-material. This indicates that some physico-chemical cross-linking between the chemical compounds of the artificial saliva solution and the ABS polymer could have occurred. If this is the case, a very particular type of cross-linking had to occur because the values of σ and E decreased for the multi-material sandwich structures after the ageing process, indicating that a normal cross-linking process did not occur.

Table C.1 of Appendix C presents the mean values obtained from multi-material specimens by Transverse Impact tests.

CONCLUSIONS

In this work, the mechanical properties of four printed mono-material polymeric specimens (ABS, HIPS, PMMA, TPU) were tested, with different infill patterns, as-printed and after aged in artificial saliva. These studies were conducted in order to understand which infill pattern would produce the best results for the mechanical properties and if the materials utilized in the printing process would be influenced by the presence of the artificial saliva solution, as to justify any disparity in results that could have appeared in the multi-material specimen test results.

It can be concluded that the presence of saliva had an impact on some of the printed mono-materials. The resilience and the absorbed energy (%) of 100% LIN ABS specimens decreased while remaining generally unchanged for other infill configurations. For 100% LIN PMMA specimens, σ decreased, and E increased, while for other infill configurations, they remained unchanged. Nonetheless, it was concluded that the infill pattern which could provide the best results for the sandwich structure would be 100%LIN, as they had the highest values for σ, E, and resilience, for all materials tested. Therefore, every sandwich specimen was printed with a 100% LIN, both skins and TPU core.

As previous works suggested, multi-material printing would be the best choice regarding the needs of the mouthguard. The mechanical properties of printed multi-material specimens were tested in non-aged and aged in artificial saliva situations as well. It can be concluded that they were not affected by the aging process globally, probably due to the presence of TPU. There was no significant variation in the mechanical properties before and after the aging process, as TPU functioned as a stabilizer for them. The impact is not as devastating since TPU composes 1/3 of the total volume of every specimen, and it was shown that TPU was not affected by the aging process.

Combining TPU with other materials negatively affected the bending properties of printed specimens, as expected, since it has very low values for these properties. Still, it was possible to reach superior results. The materials combination which presented the best bending properties were ABS-TPU-ABS and PMMA-TPU-PMMA specimens, as these present the highest values for σ while having similar results for E, even though the first

combination has a higher rigidity before the aging process. It is essential to state that there were some adherence problems in aged HIPS-TPU-HIPS specimens, as different material layers were separated during 3PB testing.

Through transverse impact testing, it was possible to acknowledge that TPU slightly improved the mechanical properties of the printed specimens while decreasing the variation in the results from each test performed (decreased standard deviations values for each sample of tested specimens). The material combination which presented the best results was ABS-TPU-ABS. While presenting the highest absorbed energy value, it also presented the highest resilience of all material combinations, one of the requirements for mouthguard integrity. The results for both aged and non-aged HIPS-TPU-HIPS and PMMA-TPU-PMMA specimens were very similar.

Overall, it is possible to conclude that the combination of materials that would suit the needs of the athlete, according to all the requirements exposed in this work, is ABS-TPU-ABS.

Further investigation can be made regarding the printing of a functioning mouthguard through FDM. The optimization of the mechanical properties of the mouthguard can be further investigated, for example, by changing some of the printed parameters, such as the infill design.

BIBLIOGRAPHY

[1] B. Lauwers, F. Klocke, A. Klink, A. E. Tekkaya, R. Neugebauer, and D. McIntosh, "Hybrid processes in manufacturing," *CIRP Ann. - Manuf. Technol.*, vol. 63, no. 2, pp. 561–583, Jan. 2014, doi: 10.1016/j.cirp.2014.05.003.

[2] *ISO/ASTM 52900(en) Additive manufacturing — General principles*. 2015.

[3] J. L. Dávila, P. I. Neto, P. Y. Noritomi, R. T. Coelho, and J. V. L. da Silva, "Hybrid manufacturing: a review of the synergy between directed energy deposition and subtractive processes," *International Journal of Advanced Manufacturing Technology*, vol. 110, no. 11. Springer Science and Business Media Deutschland GmbH, pp. 3377–3390, Oct. 01, 2020, doi: 10.1007/s00170-020-06062-7.

[4] L. Di Angelo, P. Di Stefano, and E. Guardiani, "Search for the optimal build direction in additive manufacturing technologies: A review," *Journal of Manufacturing and Materials Processing*, vol. 4, no. 3. MDPI Multidisciplinary Digital Publishing Institute, p. 71, Jul. 01, 2020, doi: 10.3390/JMMP4030071.

[5] A. Wiberg, J. Persson, and J. Ölvander, "Design for additive manufacturing – a review of available design methods and software," *Rapid Prototyp. J.*, vol. 25, no. 6, pp. 1080–1094, Jul. 2019, doi: 10.1108/RPJ-10-2018-0262.

[6] S. T. Newman, Z. Zhu, V. Dhokia, and A. Shokrani, "Process planning for additive and subtractive manufacturing technologies," *CIRP Ann. - Manuf. Technol.*, vol. 64, no. 1, pp. 467–470, Jan. 2015, doi: 10.1016/j.cirp.2015.04.109.

[7] R. Wrobel and B. Mecrow, "A Comprehensive Review of Additive Manufacturing in Construction of Electrical Machines," *IEEE Transactions on Energy Conversion*, vol. 35, no. 2. Institute of Electrical and Electronics Engineers Inc., pp. 1054–1064, Jun. 01, 2020, doi: 10.1109/TEC.2020.2964942.

[8] A. Plymill, R. Minneci, D. Alexander Greeley, J. Gritton, D. Alexander, and D. Greeley, "Graphene and Carbon Nanotube PLA Composite Feedstock Development for Fused Deposition Modeling Recommended Citation Graphene and Carbon Nanotube PLA Composite Feedstock Development for Fused Deposition Modeling," May 2016. Accessed: Oct. 27, 2020. [Online]. Available: https://trace.tennessee.edu/utk_chanhonoproj/1955.

[9] M. Keller, M. Rosenberg, M. Brettel, and N. Friederichsen, “How Virtualization, Decentrazliation and Network Building Change the Manufacturing Landscape: An Industry 4.0 Perspective,” *Int. J. Mech. Aerospace, Ind. Mechatron. Manuf. Eng.*, vol. 8, no. 1, pp. 37–44, 2014.

[10] N. Guo and M. C. Leu, “Additive manufacturing: Technology, applications and research needs,” *Frontiers of Mechanical Engineering*, vol. 8, no. 3. Springer, pp. 215–243, Sep. 08, 2013, doi: 10.1007/s11465-013-0248-8.

[11] H. Wu *et al.*, “Recent developments in polymers/polymer nanocomposites for additive manufacturing,” *Progress in Materials Science*, vol. 111. Elsevier Ltd, p. 100638, Jun. 01, 2020, doi: 10.1016/j.pmatsci.2020.100638.

[12] T. D. Ngo, A. Kashani, G. Imbalzano, K. T. Q. Nguyen, and D. Hui, “Additive manufacturing (3D printing): A review of materials, methods, applications and challenges,” *Composites Part B: Engineering*, vol. 143. Elsevier Ltd, pp. 172–196, Jun. 15, 2018, doi: 10.1016/j.compositesb.2018.02.012.

[13] O. A. Mohamed, S. H. Masood, and J. L. Bhowmik, “Optimization of fused deposition modeling process parameters: a review of current research and future prospects,” *Adv. Manuf.*, vol. 3, no. 1, pp. 42–53, Feb. 2015, doi: 10.1007/s40436-014-0097-7.

[14] B. Utela, D. Storti, R. Anderson, and M. Ganter, “A review of process development steps for new material systems in three dimensional printing (3DP),” *Journal of Manufacturing Processes*, vol. 10, no. 2. Elsevier Ltd, pp. 96–104, 2008, doi: 10.1016/j.jmapro.2009.03.002.

[15] S. Legutko, “Additive techniques of manufacturing functional products from metal materials,” in *IOP Conference Series: Materials Science and Engineering*, Aug. 2018, vol. 393, no. 1, p. 012003, doi: 10.1088/1757-899X/393/1/012003.

[16] H. Lee, C. H. J. Lim, M. J. Low, N. Tham, V. M. Murukeshan, and Y. J. Kim, “Lasers in additive manufacturing: A review,” *International Journal of Precision Engineering and Manufacturing - Green Technology*, vol. 4, no. 3. pp. 307–322, 2017, doi: 10.1007/s40684-017-0037-7.

[17] P. Yang and H. J. Fan, “Inkjet and Extrusion Printing for Electrochemical Energy Storage: A Minireview,” *Advanced Materials Technologies*, vol. 5, no. 10. Wiley-Blackwell, p. 2000217, Oct. 23, 2020, doi: 10.1002/admt.202000217.

[18] F. P. W. Melchels, J. Feijen, and D. W. Grijpma, “A review on stereolithography and its applications in biomedical engineering,” *Biomaterials*, vol. 31, no. 24. Elsevier Ltd, pp. 6121–6130, 2010, doi: 10.1016/j.biomaterials.2010.04.050.

[19] N. Travitzky *et al.*, “Additive manufacturing of ceramic-based materials,” in *Advanced Engineering Materials*, Jun. 2014, vol. 16, no. 6, pp. 729–754, doi: 10.1002/adem.201400097.

[20] Z. C. Eckel, C. Zhou, J. H. Martin, A. J. Jacobsen, W. B. Carter, and T. A. Schaedler, “Additive manufacturing of polymer-derived ceramics,” *Science (80-.).*, vol. 351, no. 6268, pp. 58–62, Jan. 2016, doi: 10.1126/science.aad2688.

[21] X. Wang, M. Jiang, Z. Zhou, J. Gou, and D. Hui, “3D printing of polymer matrix composites: A review and prospective,” *Composites Part B: Engineering*, vol. 110. Elsevier Ltd, pp. 442–458, 2017, doi: 10.1016/j.compositesb.2016.11.034.

[22] J. Z. Manapat, Q. Chen, P. Ye, and R. C. Advincula, “3D Printing of Polymer Nanocomposites via Stereolithography,” *Macromolecular Materials and Engineering*, vol. 302, no. 9. pp. 1–13, 2017, doi: 10.1002/mame.201600553.

[23] Y. S. Liao, L. C. Chiu, and Y. Y. Chiu, “A new approach of online waste removal process for laminated object manufacturing (LOM),” in *Journal of Materials Processing Technology*, Sep. 2003, vol. 140, no. 1-3 SPEC., pp. 136–140, doi: 10.1016/S0924-0136(03)00690-3.

[24] J. Park, M. J. Tari, and H. T. Hahn, “Characterization of the laminated object manufacturing (LOM) process,” *Rapid Prototyp. J.*, vol. 6, no. 1, pp. 36–49, 2000, doi: 10.1108/13552540010309868.

[25] I. Gibson, D. Rosen, and B. Stucker, *Additive manufacturing technologies: 3D printing, rapid prototyping, and direct digital manufacturing, second edition*, no. 1991. 2015.

[26] D. Pranzo, P. Larizza, D. Filippini, and G. Percoco, “Extrusion-based 3D printing of microfluidic devices for chemical and biomedical applications: A topical review,” *Micromachines*, vol. 9, no. 8. MDPI AG, p. 374, Jul. 27, 2018, doi: 10.3390/mi9080374.

[27] A. K. Sood, R. K. Ohdar, and S. S. Mahapatra, “Parametric appraisal of mechanical property of fused deposition modelling processed parts,” *Mater. Des.*, vol. 31, no. 1, pp. 287–295, Jan. 2010, doi: 10.1016/j.matdes.2009.06.016.

[28] J. S. Chohan, R. Singh, K. S. Boparai, R. Penna, and F. Fraternali, “Dimensional accuracy analysis of coupled fused deposition modeling and vapour smoothing operations for biomedical applications,” *Compos. Part B Eng.*, vol. 117, pp. 138–149, 2017, doi: 10.1016/j.compositesb.2017.02.045.

[29] P. Parandoush and D. Lin, “A review on additive manufacturing of polymer-fiber composites,” *Composite Structures*, vol. 182. Elsevier Ltd, pp. 36–53, 2017, doi: 10.1016/j.compstruct.2017.08.088.

[30] W. Kollenberg, “Ceramics and multi-material 3D printing,” *Keramische Zeitschrift*, vol. 66, no. 4. DVS Verlag, pp. 233–236, Aug. 01, 2014, doi: 10.1007/bf03400217.

[31] S. J. Park *et al.*, “Enhanced Solubility of the Support in an FDM-Based 3D Printed Structure Using Hydrogen Peroxide under Ultrasonication,” *Adv. Mater. Sci. Eng.*, vol. 2018, 2020, doi: 10.1155/2018/3018761.

[32] E. Sachs, M. Cima, and J. Cornie, “Three-Dimensional Printing: Rapid Tooling and Prototypes Directly from a CAD Model,” *CIRP Ann. - Manuf. Technol.*, vol. 39, no. 1, pp. 201–204, Jan. 1990, doi: 10.1016/S0007-8506(07)61035-X.

[33] P. Rastogi and B. Kandasubramanian, “Breakthrough in the printing tactics for stimuli-responsive materials: 4D printing,” *Chemical Engineering Journal*, vol. 366. Elsevier B.V., pp. 264–304, Jun. 15, 2019, doi: 10.1016/j.cej.2019.02.085.

[34] C. Y. Yap *et al.*, “Review of selective laser melting: Materials and applications,” *Applied Physics Reviews*, vol. 2, no. 4. American Institute of Physics Inc., p. 041101, Dec. 01, 2015, doi: 10.1063/1.4935926.

[35] H. K. D. H. Bhadeshia and R. W. K. Honeycombe, *Steels: Microstructure and Properties: Fourth Edition*. Elsevier Inc., 2017.

[36] L. Fitzsimons, G. McNamara, M. Obeidi, and D. Brabazon, *The Circular Economy: Additive Manufacturing and Impacts for Materials Processing*. 2020.

[37] N. Haghdadi, M. Laleh, M. Moyle, and S. Primig, “Additive manufacturing of steels: a review of achievements and challenges,” *Journal of Materials Science*, vol. 56, no. 1. Springer, pp. 64–107, Jan. 01, 2020, doi: 10.1007/s10853-020-05109-0.

[38] H. Fayazfar *et al.*, “A critical review of powder-based additive manufacturing of ferrous alloys: Process parameters, microstructure and mechanical properties,” *Mater. Des.*, vol. 144, pp. 98–128, Apr. 2018, doi: 10.1016/j.matdes.2018.02.018.

[39] P. Bajaj, A. Hariharan, A. Kini, P. Kürnsteiner, D. Raabe, and E. A. Jägle, “Steels in

additive manufacturing: A review of their microstructure and properties," *Mater. Sci. Eng. A*, vol. 772, p. 138633, Jan. 2020, doi: 10.1016/j.msea.2019.138633.

[40] N. Singh, P. Hameed, R. Ummethala, G. Manivasagam, K. G. Prashanth, and J. Eckert, "Selective laser manufacturing of Ti-based alloys and composites: impact of process parameters, application trends, and future prospects," *Materials Today Advances*, vol. 8. Elsevier Ltd, Dec. 01, 2020, doi: 10.1016/j.mtadv.2020.100097.

[41] J. I. Arrizubieta, O. Ukar, M. Ostolaza, and A. Mugica, "Study of the environmental implications of using metal powder in additive manufacturing and its handling," *Metals (Basel).*, vol. 10, no. 2, p. 261, Feb. 2020, doi: 10.3390/met10020261.

[42] T. Peng, K. Kellens, R. Tang, C. Chen, and G. Chen, "Sustainability of additive manufacturing: An overview on its energy demand and environmental impact," *Additive Manufacturing*, vol. 21. Elsevier B.V., pp. 694–704, May 01, 2018, doi: 10.1016/j.addma.2018.04.022.

[43] R. Chen *et al.*, "Exposure, assessment and health hazards of particulate matter in metal additive manufacturing: A review," *Chemosphere*, vol. 259. Elsevier Ltd, Nov. 01, 2020, doi: 10.1016/j.chemosphere.2020.127452.

[44] A. Majeed, A. Ahmed, J. Lv, T. Peng, and M. Muzamil, "A state-of-the-art review on energy consumption and quality characteristics in metal additive manufacturing processes," *Journal of the Brazilian Society of Mechanical Sciences and Engineering*, vol. 42, no. 5. Springer, p. 249, May 01, 2020, doi: 10.1007/s40430-020-02323-4.

[45] F. Klocke, "Modern Approaches for the Production of Ceramic Components," *J. Eur. Ceram. Soc.*, vol. 17, no. 2–3, pp. 457–465, Jan. 1997, doi: 10.1016/s0955-2219(96)00163-x.

[46] V. K. Balla, S. Bose, and A. Bandyopadhyay, "Processing of bulk alumina ceramics using laser engineered net shaping," *Int. J. Appl. Ceram. Technol.*, vol. 5, no. 3, pp. 234–242, May 2008, doi: 10.1111/j.1744-7402.2008.02202.x.

[47] E. Juste, F. Petit, V. Lardot, and F. Cambier, "Shaping of ceramic parts by selective laser melting of powder bed," *J. Mater. Res.*, vol. 29, no. 17, pp. 2086–2094, Jun. 2014, doi: 10.1557/jmr.2014.127.

[48] Y. Lakhdar, C. Tuck, J. Binner, A. Terry, and R. Goodridge, "Additive manufacturing of advanced ceramic materials," *Progress in Materials Science*, vol.

116. Elsevier Ltd, p. 100736, Feb. 01, 2021, doi: 10.1016/j.pmatsci.2020.100736.

[49] K. Ishizaki, S. Komarneni, and M. Nanko, “Powder compacts and green bodies for porous materials,” Springer, Boston, MA, 1998, pp. 12–37.

[50] A. M. Wätjen, P. Gingter, M. Kramer, and R. Telle, “Novel prospects and possibilities in additive manufacturing of ceramics by means of direct inkjet printing,” *Adv. Mech. Eng.*, vol. 2014, Feb. 2014, doi: 10.1155/2014/141346.

[51] D. H. Lee and B. Derby, “Preparation of PZT suspensions for direct ink jet printing,” *J. Eur. Ceram. Soc.*, vol. 24, no. 6, pp. 1069–1072, Jan. 2004, doi: 10.1016/S0955-2219(03)00421-7.

[52] T. Wang and B. Derby, “Ink-jet printing and sintering of PZT,” *J. Am. Ceram. Soc.*, vol. 88, no. 8, pp. 2053–2058, May 2005, doi: 10.1111/j.1551-2916.2005.00406.x.

[53] Z. Jiang, B. Diggle, M. L. Tan, J. Viktorova, C. W. Bennett, and L. A. Connal, “Extrusion 3D Printing of Polymeric Materials with Advanced Properties,” *Advanced Science*, vol. 7, no. 17. John Wiley and Sons Inc., Sep. 01, 2020, doi: 10.1002/advs.202001379.

[54] I. Cummings, E. Hillstrom, R. Newton, E. Flynn, and A. Wachtor, “In-process ultrasonic inspection of additive manufactured parts,” in *Conference Proceedings of the Society for Experimental Mechanics Series*, 2016, vol. 10, pp. 235–247, doi: 10.1007/978-3-319-30249-2_20.

[55] M. A. Caminero, J. M. Chacón, I. García-Moreno, and J. M. Reverte, “Interlaminar bonding performance of 3D printed continuous fibre reinforced thermoplastic composites using fused deposition modelling,” *Polym. Test.*, vol. 68, pp. 415–423, Jul. 2018, doi: 10.1016/j.polymertesting.2018.04.038.

[56] P. K. Penumakala, J. Santo, and A. Thomas, “A critical review on the fused deposition modeling of thermoplastic polymer composites,” *Composites Part B: Engineering*, vol. 201. Elsevier Ltd, p. 108336, Nov. 15, 2020, doi: 10.1016/j.compositesb.2020.108336.

[57] C. Hohimer, J. Christ, N. Aliheidari, C. Mo, and A. Ameli, “3D printed thermoplastic polyurethane with isotropic material properties,” in *Behavior and Mechanics of Multifunctional Materials and Composites 2017*, Apr. 2017, vol. 10165, p. 1016511, doi: 10.1117/12.2259810.

[58] G. Kim, E. Barocio, R. B. Pipes, and R. Sterkenburg, “3D printed thermoplastic

polyurethane bladder for manufacturing of fiber reinforced composites," *Addit. Manuf.*, vol. 29, p. 100809, Oct. 2019, doi: 10.1016/j.addma.2019.100809.

[59] M. Yahiaoui, J. Denape, J. Y. Paris, A. G. Ural, N. Alcalá, and F. J. Martínez, "Wear dynamics of a TPU/steel contact under reciprocal sliding," *Wear*, vol. 315, no. 1–2, pp. 103–114, Jul. 2014, doi: 10.1016/j.wear.2014.04.005.

[60] S. Kabir, H. Kim, and S. Lee, "Physical property of 3D-printed sinusoidal pattern using shape memory TPU filament," *Text. Res. J.*, vol. 90, no. 21–22, pp. 2399–2410, Nov. 2020, doi: 10.1177/0040517520919750.

[61] F. B. Koehler *et al.*, "3D printing of thermoplastic polyurethane shape memory polymer," in *CAMX 2015 - Composites and Advanced Materials Expo*, 2015, pp. 2231–2245.

[62] H. J. Qi and M. C. Boyce, "Stress-strain behavior of thermoplastic polyurethanes," *Mech. Mater.*, vol. 37, no. 8, pp. 817–839, Aug. 2005, doi: 10.1016/j.mechmat.2004.08.001.

[63] J. Xiao and Y. Gao, "The manufacture of 3D printing of medical grade TPU," *Prog. Addit. Manuf.*, vol. 2, no. 3, pp. 117–123, Sep. 2017, doi: 10.1007/s40964-017-0023-1.

[64] A. S. de León, A. Domínguez-Calvo, and S. I. Molina, "Materials with enhanced adhesive properties based on acrylonitrile-butadiene-styrene (ABS)/thermoplastic polyurethane (TPU) blends for fused filament fabrication (FFF)," *Mater. Des.*, vol. 182, Nov. 2019, doi: 10.1016/j.matdes.2019.108044.

[65] A. M. Peterson, "Review of acrylonitrile butadiene styrene in fused filament fabrication: A plastics engineering-focused perspective," *Additive Manufacturing*, vol. 27. Elsevier B.V., pp. 363–371, May 01, 2019, doi: 10.1016/j.addma.2019.03.030.

[66] J. V. Rutkowski and B. C. Levin, "Acrylonitrile–butadiene–styrene copolymers (ABS): Pyrolysis and combustion products and their toxicity—a review of the literature," *Fire Mater.*, vol. 10, no. 3–4, pp. 93–105, Sep. 1986, doi: 10.1002/fam.810100303.

[67] R. Singh, G. S. Sandhu, R. Penna, and I. Farina, "Investigations for thermal and electrical conductivity of ABS-graphene blended prototypes," *Materials (Basel).*, vol. 10, no. 8, p. 881, Jul. 2017, doi: 10.3390/ma10080881.

[68] M. Fernandez-Vicente, W. Calle, S. Ferrandiz, and A. Conejero, “Effect of Infill Parameters on Tensile Mechanical Behavior in Desktop 3D Printing,” *3D Print. Addit. Manuf.*, vol. 3, no. 3, pp. 183–192, Sep. 2016, doi: 10.1089/3dp.2015.0036.

[69] N. Markiz, E. Horváth, and P. Ficzere, “Influence of printing direction on 3D printed ABS specimens,” *Prod. Eng. Arch.*, vol. 26, no. 3, pp. 127–130, Oct. 2020, doi: 10.30657/pea.2020.26.24.

[70] A. K. Cress, J. Huynh, E. H. Anderson, R. O’neill, Y. Schneider, and Ö. Keleş, “Effect of recycling on the mechanical behavior and structure of additively manufactured acrylonitrile butadiene styrene (ABS),” *J. Clean. Prod.*, vol. 279, p. 123689, Jan. 2021, doi: 10.1016/j.jclepro.2020.123689.

[71] U. Ali, K. J. B. A. Karim, and N. A. Buang, “A Review of the Properties and Applications of Poly (Methyl Methacrylate) (PMMA),” *Polymer Reviews*, vol. 55, no. 4. Taylor and Francis Inc., pp. 678–705, Oct. 02, 2015, doi: 10.1080/15583724.2015.1031377.

[72] C. Grabowik, K. Kalinowski, G. Ćwikła, I. Paprocka, and P. Kogut, “Tensile tests of specimens made of selected group of the filament materials manufactured with FDM method,” in *MATEC Web of Conferences*, Jul. 2017, vol. 112, p. 04017, doi: 10.1051/matecconf/201711204017.

[73] F. Kotz *et al.*, “Fused Deposition Modeling of Microfluidic Chips in Polymethylmethacrylate,” *Micromachines*, vol. 11, no. 9, p. 873, Sep. 2020, doi: 10.3390/mi11090873.

[74] I. Thompson and L. L. Hench, “Medical Applications of Composites,” in *Comprehensive Composite Materials*, Elsevier, 2000, pp. 727–753.

[75] D. Espalin, K. Arcaute, D. Rodriguez, F. Medina, M. Posner, and R. Wicker, “Fused deposition modeling of polymethylmethacrylate for use in patient-specific reconstructive surgery,” in *20th Annual International Solid Freeform Fabrication Symposium, SFF 2009*, 2009, pp. 569–583.

[76] R. Singh, R. Kumar, I. Farina, F. Colangelo, L. Feo, and F. Fraternali, “Multi-material additive manufacturing of sustainable innovative materials and structures,” *Polymers (Basel).*, vol. 11, no. 1, p. 62, Jan. 2019, doi: 10.3390/polym11010062.

[77] D. M. B. Lopez and R. Ahmad, “Tensile mechanical behaviour of multi-polymer sandwich structures via fused deposition modelling,” *Polymers (Basel).*, vol. 12, no.

3, p. 651, Mar. 2020, doi: 10.3390/polym12030651.

[78] F. Soriano-Corral *et al.*, "Synthesis and characterization of high impact polystyrene from a heterogeneous styrene-rubber-polystyrene solution: Influence of PS concentration on the phase inversion, morphology and impact strength," in *Macromolecular Symposia*, Mar. 2013, vol. 325–326, no. 1, pp. 177–183, doi: 10.1002/masy.201200059.

[79] M. Kaveh, M. Badrossamay, E. Foroozmehr, and A. Hemasian Etefagh, "Optimization of the printing parameters affecting dimensional accuracy and internal cavity for HIPS material used in fused deposition modeling processes," *J. Mater. Process. Technol.*, vol. 226, pp. 280–286, Aug. 2015, doi: 10.1016/j.jmatprotec.2015.07.012.

[80] I. Gibson, D. W. Rosen, and B. Stucker, *Additive manufacturing technologies: Rapid prototyping to direct digital manufacturing*. Springer US, 2010.

[81] M. Biron, *Thermoplastics and Thermoplastic Composites (3rd Edition)*. 2018.

[82] F. Momeni, S. M.Mehdi Hassani.N, X. Liu, and J. Ni, "A review of 4D printing," *Mater. Des.*, vol. 122, pp. 42–79, May 2017, doi: 10.1016/j.matdes.2017.02.068.

[83] M. Y. Chen, J. Skewes, M. A. Woodruff, P. Dasgupta, and N. J. Rukin, "Multi-colour extrusion fused deposition modelling: a low-cost 3D printing method for anatomical prostate cancer models," *Sci. Rep.*, vol. 10, no. 1, pp. 1–5, Dec. 2020, doi: 10.1038/s41598-020-67082-7.

[84] A. K. Kaw, *Mechanics of composite materials, second edition*. 2005.

[85] I. M. Daniel and J. L. Abot, "Fabrication, testing and analysis of composite sandwich beams," in *Composites Science and Technology*, Sep. 2000, vol. 60, no. 12–13, pp. 2455–2463, doi: 10.1016/S0266-3538(00)00039-7.

[86] A. Lanzotti, M. Grasso, G. Staiano, and M. Martorelli, "The impact of process parameters on mechanical properties of parts fabricated in PLA with an open-source 3-D printer," *Rapid Prototyp. J.*, vol. 21, no. 5, pp. 604–617, Aug. 2015, doi: 10.1108/RPJ-09-2014-0135.

[87] J. M. Chacón, M. A. Caminero, E. García-Plaza, and P. J. Núñez, "Additive manufacturing of PLA structures using fused deposition modelling: Effect of process parameters on mechanical properties and their optimal selection," *Mater. Des.*, vol. 124, pp. 143–157, Jun. 2017, doi: 10.1016/j.matdes.2017.03.065.

[88] S. Brischetto, C. G. Ferro, R. Torre, and P. Maggiore, "3D FDM production and mechanical behavior of polymeric sandwich specimens embedding classical and honeycomb cores," *Curved Layer. Struct.*, vol. 5, no. 1, pp. 80–94, Apr. 2018, doi: 10.1515/cls-2018-0007.

[89] A. M. Sousa, "Avaliação das propriedades de polímeros após impressão 3D para aplicações em Protetores Bucais," p. 95, 2020.

[90] C. Berthomieu and R. Hienerwadel, "Fourier transform infrared (FTIR) spectroscopy," *Photosynthesis Research*, vol. 101, no. 2–3. pp. 157–170, Sep. 2009, doi: 10.1007/s11120-009-9439-x.

[91] D. M. Price, D. J. Hourston, and F. Dumont, "Thermogravimetry of Polymers," in *Encyclopedia of Analytical Chemistry*, Chichester, UK: John Wiley & Sons, Ltd, 2006.

[92] J. R. Davis, "Tensile Testing, 2nd Edition - ASM International," *ASM International*, 2004. https://www.asminternational.org/home/-/journal_content/56/10192/05106G/PUBLICATION (accessed Jan. 03, 2021).

[93] V. M. Ducke and N. Ilie, "Aging behavior of high-translucent CAD/CAM resin-based composite blocks," *J. Mech. Behav. Biomed. Mater.*, vol. 115, p. 104269, Mar. 2021, doi: 10.1016/j.jmbbm.2020.104269.

[94] ASTM INTERNATIONAL, "Standard Test Methods for Flexural Properties of Unreinforced and Reinforced Plastics and Electrical Insulating Materials. D790," *Annu. B. ASTM Stand.*, pp. 1–12, 2002, Accessed: Jan. 03, 2021. [Online]. Available: https://www.astm.org/Standards/D790.

[95] C. Dong and I. J. Davies, "Flexural strength of bidirectional hybrid epoxy composites reinforced by e glass and T700S carbon fibres," *Compos. Part B Eng.*, vol. 72, pp. 65–71, Apr. 2015, doi: 10.1016/j.compositesb.2014.11.031.

[96] P. N. B. dos Reis, A. M. Amaro, and M. A. Neto, "Effect of fibre orientation and hostile solutions on stress relaxation of glass/polyamide composites," *Polymers (Basel).*, vol. 12, no. 1, p. 20, Dec. 2020, doi: 10.3390/polym12010020.

[97] S. Papavinasam, *Corrosion Control in the Oil and Gas Industry*. 2013.

[98] A. F. Yee and H.-J. Sue, "Impact Resistance," in *Encyclopedia of Polymer Science and Technology*, Hoboken, NJ, USA: John Wiley & Sons, Inc., 2002.

[99] A. F. S. Leonardo, "Efeito das soluções cimentícias na resposta ao impacto

longitudinal e transversal de laminados vidro/epóxido," *Univ. Coimbra*, p. 76, 2016.

[100] A. P. Freitas, Vitor; Amaro, "Resposta ao impacto longitudinal e transversal de laminados de vidro / epóxi," *Unversity of Coimbra*, 2016.

[101] ISO 179-1, "Plastics — Determination of Charpy impact properties — Part 1: Non-instrumented impact test," no. 1110. p. 22, 2010, Accessed: Jan. 03, 2021. [Online]. Available: https://www.iso.org/standard/44852.html.

[102] R. Marques Chaves, "Mechnical Properties of Recycled Polymers after 3D Printing," *Univ. Coimbra*, 2019.

[103] A. S. Niknejad, S. Bazgir, A. Sadeghzadeh, and M. M. A. Shirazi, "Evaluation of a novel and highly hydrophobic acrylonitrile-butadiene-styrene membrane for direct contact membrane distillation: Electroblowing/air-assisted electrospraying techniques," *Desalination*, vol. 500, p. 114893, Mar. 2021, doi: 10.1016/j.desal.2020.114893.

[104] S. Khoshnevisan and S. Bazgir, "Treatment of dye wastewater by direct contact membrane distillation using superhydrophobic nanofibrous high-impact polystyrene membranes," *Int. J. Environ. Sci. Technol.*, pp. 1–16, Aug. 2020, doi: 10.1007/s13762-020-02894-8.

[105] E. Moradi, H. Ebrahimzadeh, and Z. Mehrani, "Electrospun acrylonitrile butadiene styrene nanofiber film as an efficient nanosorbent for head space thin film microextraction of polycyclic aromatic hydrocarbons from water and urine samples," *Talanta*, vol. 205, p. 120080, Dec. 2019, doi: 10.1016/j.talanta.2019.06.080.

[106] G. Wypych, *Handbook of Polymers: Second Edition*. 2016.

[107] N. K. Cummins and I. R. Spears, "The effect of mouthguard design on stresses in the tooth-bone complex," *Med. Sci. Sports Exerc.*, vol. 34, no. 6, pp. 942–947, 2002, doi: 10.1097/00005768-200206000-00006.

[108] K. Kim, J. Park, J. hoon Suh, M. Kim, Y. Jeong, and I. Park, "3D printing of multiaxial force sensors using carbon nanotube (CNT)/thermoplastic polyurethane (TPU) filaments," *Sensors Actuators, A Phys.*, vol. 263, pp. 493–500, Aug. 2017, doi: 10.1016/j.sna.2017.07.020.

[109] ASTM International, "ASTM F697-00: Standard Practice for Care and Use of Athletic Mouth Protectors," 2000. https://www.astm.org/Standards/F697.htm

(accessed Jan. 03, 2021).

[110] C. H. Ferrari and J. M. Ferreira De Medeiros, “Dental trauma and level of information: Mouthguard use in different contact sports,” *Dent. Traumatol.*, vol. 18, no. 3, pp. 144–147, Jun. 2002, doi: 10.1034/j.1600-9657.2002.00017.x.

[111] “Using mouthguards to reduce the incidence and severity of sports-related oral injuries,” *J. Am. Dent. Assoc.*, vol. 137, no. 12, pp. 1712–1720, 2006, doi: 10.14219/jada.archive.2006.0118.

[112] J. J. Knapik, B. L. Hoedebecke, G. G. Rogers, M. A. Sharp, and S. W. Marshall, “Effectiveness of Mouthguards for the Prevention of Orofacial Injuries and Concussions in Sports: Systematic Review and Meta-Analysis,” *Sports Medicine*, vol. 49, no. 8. Springer International Publishing, pp. 1217–1232, Aug. 01, 2019, doi: 10.1007/s40279-019-01121-w.

[113] A. M. Sousa, A. C. Pinho, A. Messias, and A. P. Piedade, “Present status in polymeric mouthguards. A future area for additive manufacturing?,” *Polymers*, vol. 12, no. 7. MDPI AG, pp. 1–18, Jul. 03, 2020, doi: 10.3390/polym12071490.

[114] I. Suhariadi, M. Shiratani, and N. Itagaki, “Morphology Evolution of ZnO Thin Films Deposited by Nitrogen Mediated Crystallization Method,” in *MATEC Web of Conferences*, Mar. 2018, vol. 159, doi: 10.1051/matecconf/201815902031.

APPENDIX A – GEOMETRY OF PRINTED SPECIMENS FOR TESTING

Table A. 1. Mean average values and standard deviation of the geometry of printed specimens for the 3PB test.

Material	Infill	Length (mm)	Width (mm)	Depth (mm)
ABS	15% 3D	59.7*	9.9 ± 0.1	2.1*
	15% HEX	59.7 ± 0.1	9.9*	2.2*
	100% LIN	59.9 ± 0.1	10.0*	2.1*
HIPS	15% 3D	59.7 ± 0.1	9.9*	2.1*
	15% HEX	59.7*	9.9*	2.0*
	100% LIN	59.7*	10.0*	2.1*
PMMA	15% 3D	59.8*	9.9*	2.1*
	15% HEX	59.7*	9.9*	2.2 ± 0.1
	100% LIN	59.9*	10.1*	2.2*
TPU	100% LIN	60.0 ± 0.2	10.4 ± 0.2	2.1 ± 0.2
ABS-TPU	100% LIN	60.3 ± 0.1	10.3 ± 0.1	2.4 ±*
HIPS-TPU	100% LIN	60.3 ± 0.1	10.4*	2.5 ±*
PMMA-TPU	100% LIN	60.2 ± 0.1	10.3*	2.4 ±*

* Values with standard deviation of 0.0

Table A. 2. Mean average values and standard deviation of the geometry of printed specimens for the transverse impact test.

Material	Infill	Length (mm)	Width (mm)	Depth (mm)
ABS	15% 3D	79.6 ± 0.1	9.9*	2.1*
	15% HEX	79.5*	9.9*	2.0*
	100% LIN	79.6*	9.9*	2.1*
HIPS	15% 3D	79.5 ± 0.1	9.9*	2.0*
	15% HEX	79.5 ± 0.1	9.9*	2.1*
	100% LIN	79.5*	9.9*	2.1*
PMMA	15% 3D	79.6*	9.9*	2.0*
	15% HEX	79.6*	10.0*	2.0*
	100% LIN	79.8*	10.2 ± 0.1	2.2*
TPU	100% LIN	80.2 ± 0.1	10.5 ± 0.3	2.1 ± 0.1
ABS-TPU	100% LIN	84.1 ± 0.1	10.8*	2.4*
HIPS-TPU	100% LIN	84.2 ± 0.2	11.0 ± 0.1	2.5*
PMMA-TPU	100% LIN	84.0 ± 0.1	10.8 ± 0.1	2.4*

* Values with standard deviation of 0.0

APPENDIX B – 3 POINT BENDING TEST

Table B. 1. Mean average values and standard deviation of the results from 3PB testing.

Specimen	Infill	Aging	σ (MPa)	E (GPa)
ABS	15% 3D	Aged	26.5 ± 1.2	0.9*
		Non-aged	25.8 ± 1.0	0.9*
	15% HEX	Aged	26.0 ± 1.2	1.0*
		Non-aged	26.6 ± 1.8	0.9*
	100% LIN	Aged	44.5 ± 0.6	1.3 ± 0.1
		Non-aged	45.6 ± 0.5	1.3 ± 0.1
HIPS	15% 3D	Aged	5.9 ± 0.6	0.8*
		Non-aged	9.5 ± 0.5	0.8 ± 0.1
	15% HEX	Aged	15.8 ± 1.1	1.0*
		Non-aged	11.4 ± 0.5	1.0 ± 0.1
	100% LIN	Aged	21.1 ± 1.3	1.2 ± 0.1
		Non-aged	17.8 ± 0.3	1.2 ± 0.1
PMMA	15% 3D	Aged	20.2 ± 2.7	0.8*
		Non-aged	25.4 ± 0.7	0.6*
	15% HEX	Aged	23.5 ± 3.9	0.8 ± 0.1
		Non-aged	23.0 ± 5.0	0.6 ± 0.2
	100% LIN	Aged	32.4 ± 2.1	1.0 ± 0.1
		Non-aged	37.7 ± 1.2	0.9 ± 0.1
TPU	100% LIN	Aged	1.3 ± 0.4**	25.4 MPa
		Non-aged[1]	1.05 ± 0.2	18 MPa
ABS-TPU	100% LIN	Aged	29.5 ± 1.4	0.6*
		Non-aged	31.0 ± 0.6	0.8 ± 0.1
HIPS-TPU	100% LIN	Aged	13.4 ± 1.9	0.7 ± 0.1
		Non-aged	15.4 ± 0.9	0.7*
PMMA-TPU	100% LIN	Aged	21.6 ± 0.5	0.5*
		Non-aged	28.8 ± 1.8	0.6*

σ – Bending Stress; ***E*** – Bending Elastic Modulus; *values with standard deviation of 0.0; **stress at the end of the test; [1] – results from previous works.

APPENDIX C – TRANSVERSE IMPACT TESTING

Table C. 1. Mean average values and standard deviation of the results from transverse impact testing.

Specimen	Infill	Aging	Absorbed Energy (%)	Resilience ($kJ.m^{-2}$)	Energy (J)
ABS	15% 3D	Aged	5.7 ± 0.3	14.3 ± 0.8	0.3*
		Non-aged	5.7 ± 0.2	14.3 ± 0.6	0.3*
	15% HEX	Aged	5.5 ± 0.5	13.8 ± 1.1	0.3*
		Non-aged	6.0 ± 0.7	15.1 ± 1.8	0.3*
	100% LIN	Aged	5.7 ± 0.3	14.4 ± 0.8	0.3*
		Non-aged	8.0 ± 1.2	20.1 ± 3.0	0.4 ± 0.1
HIPS	15% 3D	Aged	3.3 ± 0.4	8.2 ± 1.1	0.2*
		Non-aged	3.2 ± 0.5	8.1 ± 1.2	0.2*
	15% HEX	Aged	2.9 ± 0.4	7.2 ± 0.9	0.1*
		Non-aged	3.5 ± 0.6	8.8 ± 1.4	0.2*
	100% LIN	Aged	6.6 ± 0.1	16.4 ± 0.3	0.3*
		Non-aged	5.6 ± 0.2	14.1 ± 0.5	0.3*
PMMA	15% 3D	Aged	2.8 ± 0.3	7.1 ± 0.8	0.1*
		Non-aged	2.7 ± 0.4	6.8 ± 1.0	0.1*
	15% HEX	Aged	2.4 ± 0.9	6.0 ± 2.3	0.1*
		Non-aged	3.5 ± 0.8	8.7 ± 1.9	0.2*
	100% LIN	Aged	6.0 ± 0.8	15.0 ± 2.1	0.3*
		Non-aged	5.3 ± 1.0	13.2 ± 2.4	0.3*
TPU	100% LIN	Aged	0.2 ± 0.2	3.0 ± 0.4	0.1*
		Non-aged[1]	0.9 ± 0.2	2.2 ± 0.4	0.04*
ABS-TPU	100% LIN	Aged	8.9 ± 0.2	22.2 ± 0.5	0.4*
		Non-aged	8.9 ± 0.4	22.4 ± 1.1	0.4*
HIPS-TPU	100% LIN	Aged	5.5 ± 0.2	13.9 ± 0.4	0.3*
		Non-aged	6.1 ± 0.1	15.2 ± 0.2	0.3*
PMMA-TPU	100% LIN	Aged	6.5 ± 0.6	16.3 ± 1.6	0.3*
		Non-aged	6.3 ± 0.4	15.8 ± 0.9	0.3*

*values with standard deviation of 0.0; [1] – results from previous works.

APPENDIX D – MORPHOLOGY OF SPECIMENS

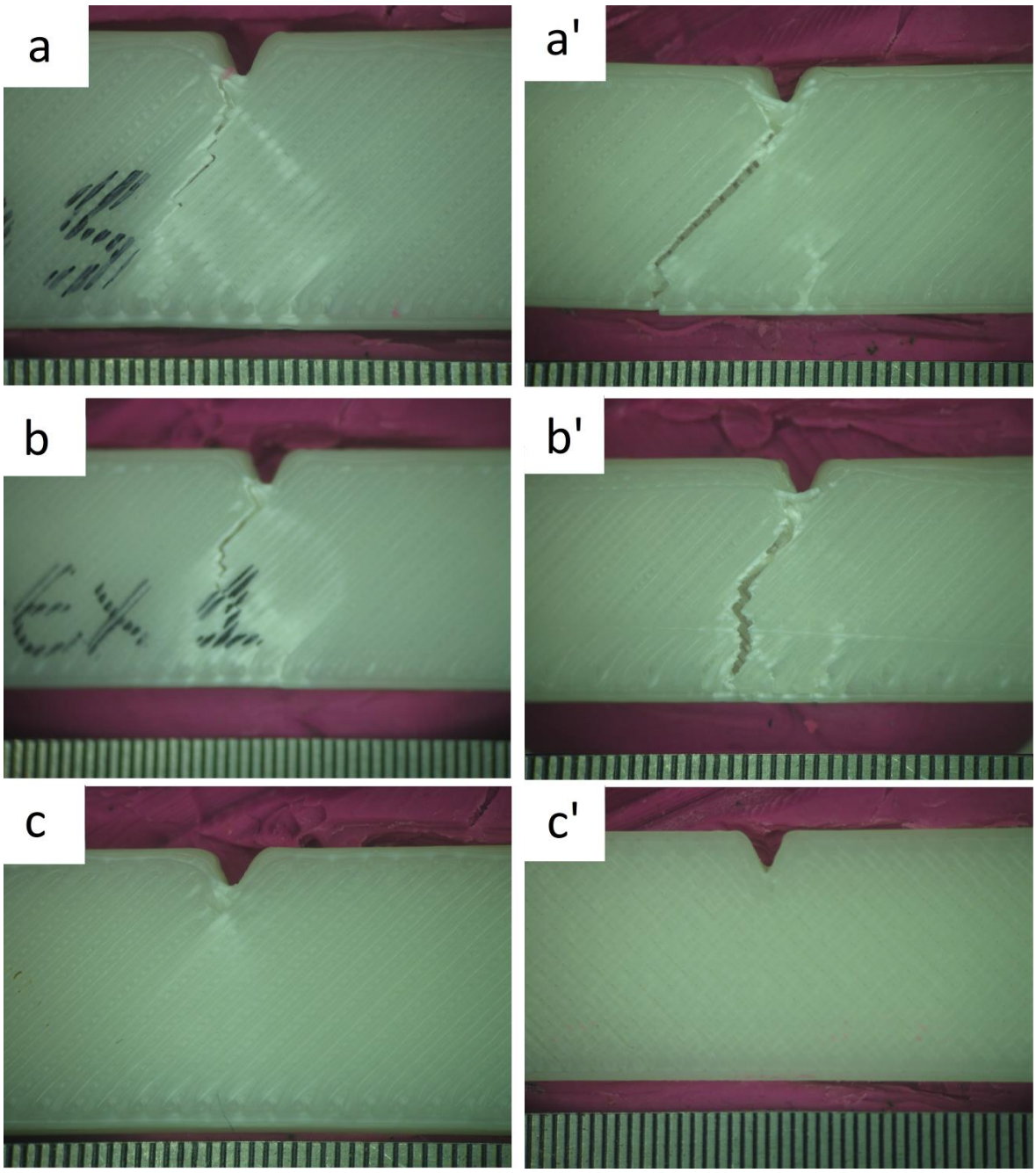

Figure D. 1. Morphology of the damage and fracture after impact on printed ABS specimens: a) 15% 3D; a') 15% 3D aged; b) 15% HEX; b') 15% HEX aged; c) 100%LIN; c') 100%LIN aged. Step is 1 mm.

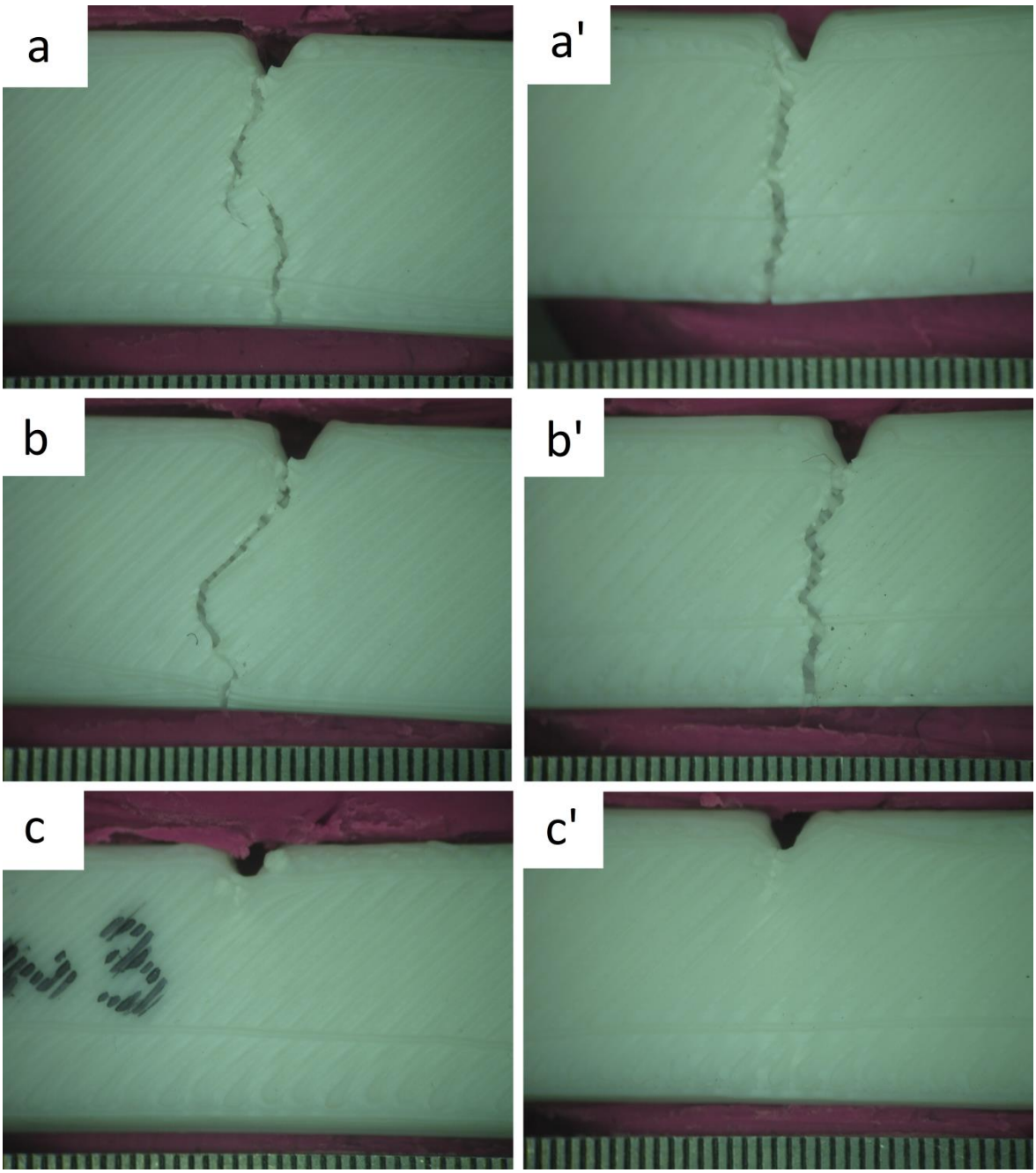

Figure D. 2. Morphology of the damage and fracture after impact on printed HIPS specimens: a) 15% 3D; a') 15% 3D aged; b) 15% HEX; b') 15% HEX aged; c) 100%LIN; c') 100%LIN aged. Step is 1 mm.

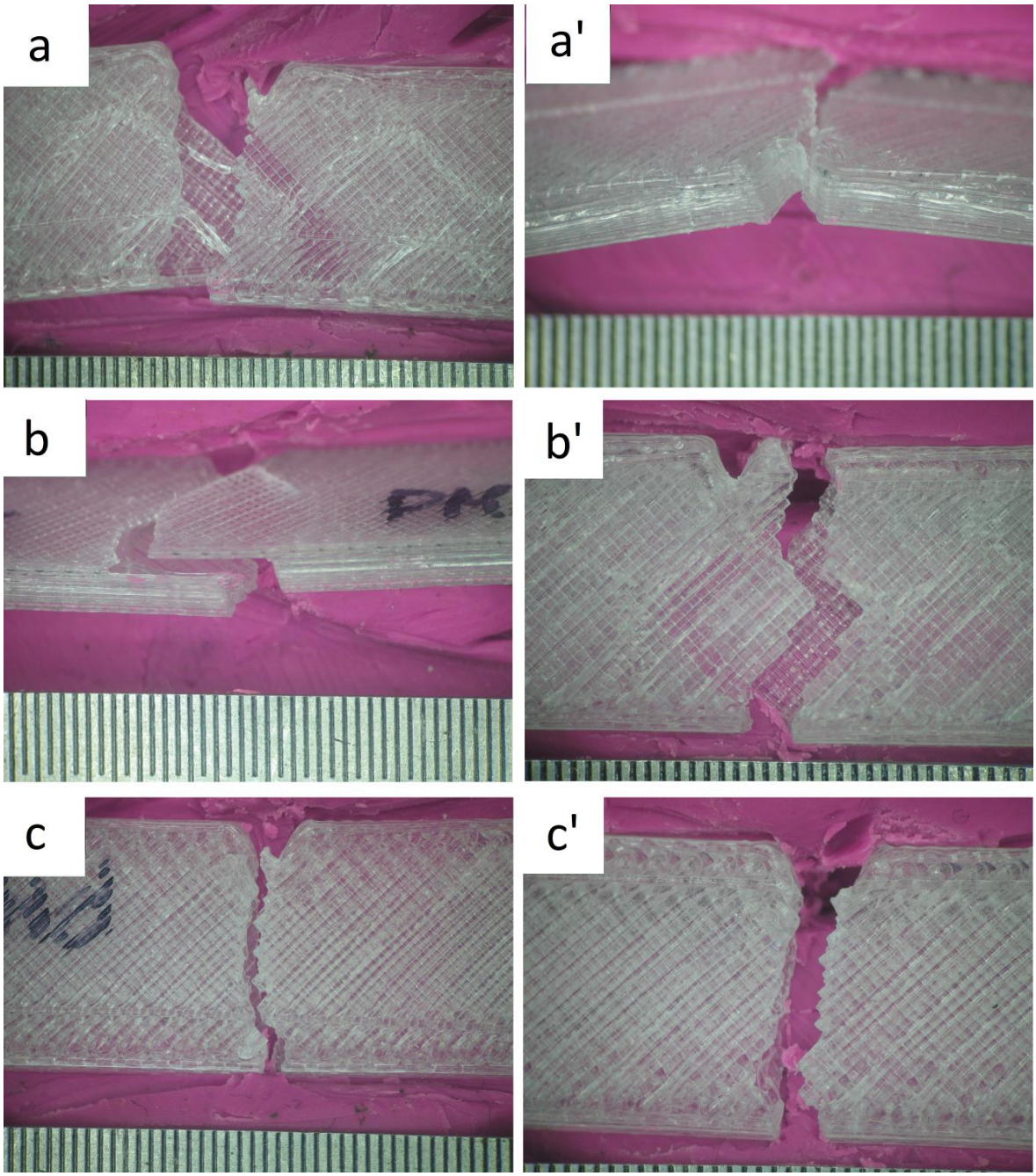

Figure D. 3. Morphology of the damage and fracture after impact on printed PMMA specimens: a) 15% 3D; a') 15% 3D aged; b) 15% HEX; b') 15% HEX aged; c) 100%LIN; c') 100%LIN aged. Step is 1 mm.

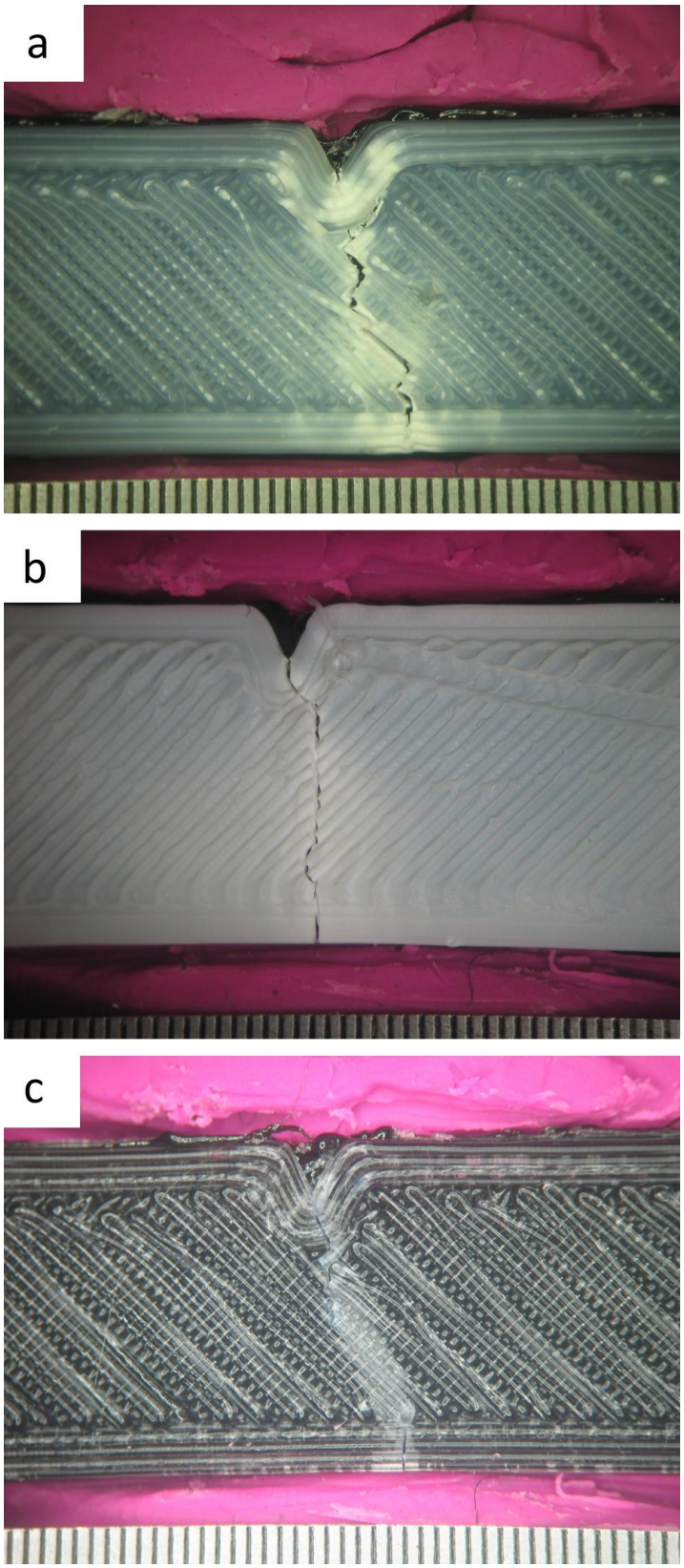

Figure D. 4. Morphology of the damage and fracture after impact on printed multi-material sandwich specimens: a) ABS-TPU-ABS; b) HIPS-TPU-HIPS; c) PMMA-TPU-PMMA. Step is 1 mm.